CANADIAN THESES

THÈSES CANADIENNES

NOTICE

The quality of this microfiche is heavily dependent upon the quality of the original thesis submitted for microfilming. Every effort has been made to ensure the highest quality of reproduction possible.

If pages are missing, contact the university which granted the degree.

Some pages may have indistinct print especially if the original pages were typed with a poor typewriter ribbon or if the university sent us an inferior photocopy.

Previously copyrighted materials (journal articles, published tests, etc.) are not filmed.

Reproduction in full or in part of this film is governed by the Canadian Copyright Act, R.S.C. 1970, c. C-30.

AVIS

La qualité de cette microfiche dépend grandement de la qualité de la thèse soumise au microfilmage. Nous avons tout fait pour assurer une qualité supérieure de reproduction.

S'il manque des pages, veuillez communiquer avec l'université qui a conféré le grade.

La qualité d'impression de certaines pages peut laisser à désirer, surtout si les pages originales ont été dactylographiées à l'aide d'un ruban usé ou si l'université nous a fait parvenir une photocopie de qualité inférieure.

Les documents qui font déjà l'objet d'un droit d'auteur (articles de revue, examens publiés, etc.) ne sont pas microfilmés.

La reproduction, même partielle, de ce microfilm est soumise à la Loi canadienne sur le droit d'auteur, SRC 1970, c. C-30.

THIS DISSERTATION
HAS BEEN MICROFILMED
EXACTLY AS RECEIVED

LA THÈSE A ÉTÉ
MICROFILMÉE TELLE QUE
NOUS L'AVONS REÇUE

A MAP/IMAGE CONGRUENCY EVALUATION KNOWLEDGE BASED SYSTEM

by

G.W. PLUNKETT

JUNE, 1986

A thesis
presented to the University of Ottawa
in partial fulfillment of the
requirements for the degree of
Master of Applied Sciences
in
Electrical Engineering

Ottawa, Ontario, CANADA

ISBN 0-315-33299-9

ABSTRACT

The fully automated integration of remotely sensed data with Geographic Information Systems (GIS) data is a formidable endeavor. One source of the difficulty is the spatial incongruency of these disparate data sets. The first step in any automated integration paradigm is to evaluate the spatial congruency of the remote sensing (imagery) data and the cartographic (map) data, to determine where the imagery elements and the corresponding map elements are in the same location, and where they are not.

This thesis describes the design, implementation and assessment of an experimental Map/Image Congruency Evaluation (MICE) knowledge based system (KBS) for investigating the spatial congruency of cartographic data and remotely sensed images. The MICE KBS consists of the execution of a number of preprocessing stages for both the map and the image to a uniform representation of the data. The PROLOG KBS then selects and executes appropriate rules from the knowledge base in order to evaluate the spatial congruency of the map and the image. Further post-processing stages transform the results into image format for human interpretation. An experiment using geocoded Landsat Multispectral Scanner (MSS) data and forest cover inventory cartographic data is presented. Favourable results, conclusions and further work related to this experiment are reported.

CONTENTS

TABLE OF CONTENTS

CONTENTS

LIST OF FIGURES

CONTENTS

LIST OF TABLES

ACKNOWLEDGMENTS

First, I would like to thank Dr. Morris Goldberg, my thesis supervisor, for his direction, guidance and advice. His timely supply of reference material was always conducive to new concepts. Also, I would like to thank him for starting myself and others down the road of Perception Research using Artificial Intelligence techniques.

Next, I would like to thank my wife Joy and my family (Shawn, Robyn and Adam) for their patience and understanding in the course of the generation of this thesis.

Next, I would like to thank Dr. David Goodenough of CCRS for allowing me to perform most of this research using the CCRS computing facilities. Also, I would like to thank him for his encouragement and support during the thesis research, for which, I will always be appreciative.

Finally, I would like to thank Francois Braun for his original labour on the Remote Sensing Expert System Shell, and to Gerald Karam for his additional work and enhancements to the Shell. Also, I would like to thank all my colleagues in the Methodology Section of CCRS for their enlightening discussions and for sharing their knowledge.

LIST OF TERMS

- AI	Artificial Intelligence
- BC	British Columbia
- BCMF	British Columbia Ministry of Forests
- CCRS	Canada Centre For Remote Sensing
- CCT	Computer Compatible Tape
- DICS	Digital Image Correction System
- GIS	Geographic Information System
- KBS	Knowledge Based System
- MICE	Map/Image Congruency Evaluation System
- MSS	Multispectral Scanner
- NASA	National Aeronautics and Space Administration
- NOAA	National Oceanic and Atmospheric Administration
- RESHELL	Remote Sensing Expert System Shell
- RMS	Root Mean Square
- UTM	Universal Transverse Mercator Projection

1 INTRODUCTION

Remotely sensed data, particularly from the LANDSAT series of satellites, are being used for a wide variety of useful applications. One of the more challenging applications is the integration of remotely sensed data with cartographic data bases, for data input or update purposes. It was found that algorithmic data integration paradigms do not provide satisfactory results, in part, due to various geometric differences between the remote sensing data and the cartographic data. These spatial incongruencies could be due to factors such as temporal differences between the data, planimetric errors in the map data or topographic effects in the remote sensing data. This thesis will report on the design, implementation and evaluation of a system for determining the spatial congruency of maps and images, irregardless of the source of any incongruency.

Some reseachers have investigated the use of knowledge based systems for performing visual tasks such as image understanding, scene interpretations and map guided air photo interpretation. Promising results have been reported on this research. A knowledge based system approach was selected as the research tool for performing the map/image congruency evaluation, since algorithmic techniques are not robust enough in this particular application, and since there have been promising results reported using a knowledge based approach for related tasks.

The Map/Image Congruency Evaluation (MICE) Knowledge Based System (KBS) was designed, implemented and evaluated for determining the spatial agreement of features in a map with the corresponding features in a remotely sensed image. The congruency evaluation paradigm includes three basic stages. These stages are:

1. An input and preprocessing stage, where both the image data and the map data are converted to a uniform symbolic representation and object attribution is performed;

2. A rule-based stage, where spatial reasoning on the symbolic image and map data using codified knowledge and deductive reasoning is executed;

3. A postprocessing and output stage, which converts the symbolic congruency evaluation results into iconic form for human interpretation.

The MICE system was evaluated using cartographic information from a British Columbia Ministry of Forests (BCMF) forest cover map, which was stored digitally as vector iconic data in a Universal Transverse Mercator (UTM) projection. Various features from this digital map were selected and rasterized to a square grid. Several properties of all the map segments contained in the features were determined. These segment properties, such as size, shape and location, were codified into a symbolic

map properties file as object attributes.

The LANDSAT data used for MICE evaluation, was geocoded by the Canada Centre for Remote Sensing (CCRS) Digital Image Correction System (DICS) to a UTM projection coordinate grid. The sub-area of the LANDSAT image corresponding to the BCMF forest cover map was selected. The Landsat image was then segmented to highlight the various features that were selected from the map. Numerous properties of the image segments, such as the segment shape, size, location and spectral means, were evaluated. These properties were codified into symbolic image properties files as object attributes.

The rule-based stage read the symbolic map attributes file and the symbolic image attributes files and evaluated the spatial congruency of the map and the image segments by reasoning about the various segment attributes. The identification of each image segment class was deduced, in order to determine if the spatially corresponding map segment belongs to the same class as the image segment. For instance, a segment selected from the hydrography feature level of the map should correspond to a segment in the image that has a spectral signature that corresponds to hydrography. If the Landsat segment does not have a corresponding spectral signature, then the segment is only weakly classified. Also, the image segments that have similar size, similar shape and spatial overlap with each map segment are deduced. Finally, the exact location of

the image segments that match the spatially corresponding map segment, is output to a symbolic results file. Following the successful completion of the rule-based stage, the results files are converted from symbolic format to imagery format, which may be displayed for human interpretation and evaluation.

The results of the current research are quite favourable for comparing maps and images using a knowledge based system approach. The MICE system was able to identify and compare the majority of the features identified in the map. The major problem area is in the segmentation and identification of small image segments. This problem is caused by the small segment size, as compared to the fairly large spatial resolution of the MSS data. This problem may be resolved by using higher spatial resolution data such as Landsat Thematic Mapper (TM) data. Additionally, more rules regarding the segment classification could enhance the systems performance.

This thesis is organized as follows. Following this intoductory chapter, Chapter 2 discusses the various domain knowledge that is pertinent to the design of the MICE KBS. Next, Chapter 3 outlines some of the important issues related to the design and implementation of Expert and Knowledge based systems. Chapter 4 is concerned with the problems of integrating remote sensing data into geographic information systems. Given these integration problems, Chapter 5 discusses the design issues of this KBS, which

attempts to solve some of these problems. Next, Chapter 6 outlines the implementation of the entire system, from the preprocessing through the rule based stage to the postprocessing stage. Chapter 7 elaborates on a demonstration experiment and reviews the results. Finally Chapter 8 provided the summary and conclusions on the KBS and the experiment.

2 THE DOMAIN

2.1 WHAT IS REMOTE SENSING?

Remote sensing is the study of objects or areas from a distance. The term "remote sensing" also often refers to the detection, recording and analysis of electromagnetic radiation. Civilian satellite remote sensing began in 1972, when the United States National Aeronautics and Space Administration (NASA), through the Earth Resources Survey Program, launched the Landsat 1 satellite (originally named the Earth Resources Technology Satellite or ERTS-1). Several additional satellites have been launched since then, with the most recent being Landsat-5.

One of the sensors on the Landsat-5 mission is the multispectral scanner (MSS). The MSS sensor receives from the earth reflected electromagnetic radiation which is transferred by a series of mirrors through filters that are selected to pass certain wavelength intervals. The filtered energy is detected, digitized and transmitted back to earth. The digitized signals are received and recorded on high density magnetic tapes at an earth receiving station. The digital video data may then be reformatted and precision geocoded onto a computer compatible tape (CCT) for analysis. Additional technical descriptions of the Landsat MSS sensor is available in the references [NASA83] [NOAA84]. Additional technical information on the reformatting and geocoding done by CCRS is also available

in the references [MURPHY83] [GUERTIN81].

The principle behind spectral analysis of the MSS data stems from the basic physical properties of materials, in that each material reflects different amounts of electromagnetic radiation at different wavelengths. Thus various materials can be separated and possibly identified by analyzing the reflectance characteristics or spectral signatures received from the sensor. For example vegetation typically reflects more green light that red light and is usually very reflective in the infrared region of the spectrum. In addition, spatial properties, such as texture may be used to aid in the identification of various materials.

Precision geocoding is the term used when the remotely sensed data is spatially rectified to conform to a specified geographic reference system. In Canada, the geocoded MSS product from CCRS is rectified to a UTM projection with 50x50 metre pixels. This product is generated by locating several corresponding control points in the uncorrected image and in a UTM projection map. These control points are then used to calculate the coefficients of a transformation function. Finally the geocoded image is generated by resampling the pixels in the original image at each point required in the geocoded image. This product has been shown to be quite accurate geometrically and is suitable for data integration into a geographic information system. An error analysis of the

geocoded product is given in the references [GUERTIN81].

In the Landsat image there can be a number of anomalies and error sources. These errors are usually defined generically as spectral and spatial errors. Although many of these errors can be reduced or eliminated using conventional mathematical modeling algorithms, some can not. It is essential then, that a rule based system for congruency evaluation purposes, be aware of these error sources as the modeling algorithms themselves may introduce other errors or anomalies.

The sources of major spectral and spatial errors in Landsat data, and what the MICE KBS assumes about these errors are:

1. Atmospheric effects such as clouds, cloud shadows and haze. These sources are typically random and difficult (or impossible) to correct. These errors are for the moment ignored, but rules for identifying clouds, haze and cloud shadows could be added at a later date.

2. The radiance received at the sensor is comprised of target radiance plus path radiance, which includes radiation scattered to the sensor and radiation reflected from adjacent targets [WOODHAM85]. These errors are currently ignored.

3. Surface topology causes changes in the reflected energy due to varying incident energy angles. This is quite a serious problem for target identification, as the reflected energy of a target (forest for example) on a flat surface has different characteristics than the reflected energy of the same target viewed from a sloped surface, such as the side of a mountain. These errors are currently ignored by assuming that the targets are Lambertian reflectors.

4. Sensor effects due to the mirror, optics and detectors cause various spectral and spatial errors. These errors are compensated for in the preprocessing stage before geocoding and are ignored.

5. Spacecraft effects caused by the multiplexing, quantization and transmission of the sensed data. These errors may cause noise or dropouts and are currently ignored.

6. Spacecraft effects from changes in the position, attitude and altitude cause geometric anomalies. These effects, which are usually slowly varying, are normally reduced during geocoding and are ignored.

7. Ground segment effects from the detection, processing and recording of the sensed data. These effects are normally minimal, but they may cause noise in the image or dropped out lines. For MICE analysis, these errors are ignored.

8. Processing effects from the transcription, correction and rectification of the data. These effects have been shown to be quite small (ie less than a half pixel geometric error) and are ignored.

CCRS has addressed a large number of these error sources, and produces a UTM projection geocoded product that has subpixel geometric accuracy. Since an algorithmic procedure has been developed to correct the MSS data to a known projection, it is essentially unnecessary for the knowledge based system to attempt to perform this correction. For the above reasons, the MICE system was developed to make use of the CCRS geocoded MSS product. At the moment MICE does not detect clouds, haze, cloud/haze shadow or line/pixel dropouts. Detection and correction of these error sources could be added during a later stage of development.

2.2 WHAT IS A GEOGRAPHIC INFORMATION SYSTEM?

A Geographic Information System (GIS) is defined as [MARBLE84]: "Applying computer technology to the problem of storing, manipulating and analyzing large volumes of spatial data... These geographic information systems comprise some quite sophisticated computer software, but they all contain the following major components:

1. A data input subsystem....
2. A data storage and retrieval subsystem...
3. A data manipulation and analysis subsystem...
4. A data reporting subsystem..."

There is no question about the high value of GIS data bases in Canada. In this information society, it is essential to have the capability of retrieving and generating maps or other presentations on various geographic and thematic elements, quickly and easily. One such GIS is used and operated by the Inventory Branch of the British Columbia Ministry of Forests (BCMF). " BCMF is required to develop, compile and maintain the inventory of the forest resources over an area of approximately 52 million hectares, including the management of the data base, the annual update of the resource maps and the associated files, and the continuous monitoring of forest depletion" [HEGYI83].

As with any technology, there are several problems associated with any GIS. One of the major problems is the data base updating, at minimum cost with maximum quality data. BCMF have a major updating problem, as this very large data base must be updated annually, as required by BC law. To meet this end, BCMF have been looking to the remote sensing community for support. The Landsat series of satellites have been useful in providing the information required for the updating, due to the large area coverage and timeliness of the data. The technique of extracting information from the remote sensing data (such as Landsat) and entering the information into a GIS is called "data integration".

Data integration has been defined as: "The process of registering discrete and spatially distributed sensor data sets and ancillary data bases in a manner which accounts for measurement incongruencies and provides spatially comparable data sets" [BRYANT82]. At BCMF, this data integration is done by performing spectral analysis on a remotely sensed image to locate classes of interest, such as forest clear cuts or fire burns. The outlines of these classified areas are then placed in the GIS database. The problem occurs when there is spatial incongruency between the classified areas and the GIS database. It has been shown that the automatic insertion of the classified area into the database is not feasible as there are often spatial difference between the map and the image data

[GOODENOUGH85].

Another problem associated with GIS systems is the large investment in existing data. Cartographers input data into a GIS using various photogrammetric techniques and often there is reluctance to change the data base once input, even though it is known to be incorrect. Often, the data integration elements are moved to a location where it "fits" into the map, rather than changing the locations or shapes of existing elements, or changing the base map.

This means that even though the remote sensing image is rectified to the same projection as the cartographic data, there are likely to be random non-linear spatial discrepancies between the map and the image data. This causes problems during data integration, because the classified image elements cannot be inserted directly into the GIS database, based only on its spatial position.

Algorithmic techniques have been used in the integration problem, with limited success [PARSONS84]. Billingsley indicated: "The essence of the process simply is that maps and images do not cross-correlate very neatly in a computer, as maps and features in images look different" [BILLINGSLEY82].

For these reasons mathematical algorithms do not provide satisfactory results to the integration problem and hence there is potential for the use of artificial intelligence techniques in a rule-base system for

performing the data integration. The first step in the data integration paradigm is simply to evaluate the spatial differences and to try to quantify these differences. This is the purpose of the MICE KBS: to evaluate the spatial agreement of features in an image with corresponding features in a map, using a knowledge based system approach.

2.3 WHAT IS PHOTOGRAMMETRY?

Photogrammetry is the science of the transformation of photographs into maps. Most GIS systems today, contain map data that was collected, analysed and input using photogrammetric techniques. Older paper maps, that were generated manually, may be digitized and put into a GIS system [BOYLE80]. In order to understand the nature of errors in a GIS, it is necessary to review some of these photogrammetric techniques.

Photogrammetric data acquisition usually requires taking air photos with precise altitude, attitude and positional information. The photos are then developed, indexed and mosaiced using geodetic control points. The map is usually then generated by manually tracing desired features from the air-photo mosaic. The output of the tracing may go directly into a GIS (digitization) or onto hardcopy (scribing).

There are a number of differences between a map and a photograph, which must be taken into account when analyzing air photos. These differences are:

1. maps are drawn to a predetermined scale.

2. maps display only selected features, depending on the purpose of the map.

3. maps emphasize certain selected features.

4. maps display features using standard symbols.

5. maps are generalized (ie some detail is lost).

6. maps are lettered, titled and labeled.

7. maps are produced based on some standard projection.

When tracing an air photo mosaic, the photo interpreter must use considerable judgment in identifying the features of interest from the photo. Some of the clues used by air-photo interpreters in feature identification are as follows:

1. The relative size of the feature can be determined mentally or a more quantitative size value can be determined by direct measurement.

2. The shape of the feature is determined. Usually natural features have irregular shapes and man-made features have regular outlines.

3. The tone or colour of the feature is assessed.

4. The texture of the feature is assessed to determine its pattern.

5. Any shadows in the photograph will give an indication of the height (or depth) of a feature.

6. Many man-made features have visible approaches, such as driveways for houses or railways for factories.

7. Relationships (or adjacency [SHAPIRO80]) give a clue to feature identification (ie a road crossing a river would be a bridge).

8. Stereoviewing allows humans to mentally generate a 3-dimensional understanding from two 2-dimensional images. This often will give a clue to feature identification.

Most of these feature identification clues are so obvious to humans that they are often "second nature". However, each of these clues adds essential information to the feature identification problem in an expert system. In addition, all of the techniques used for air-photo interpretation are the same as for satellite-photo or satellite image interpretation, except that the relative scale of the images is different.

3 WHAT IS AN EXPERT SYSTEM?

Artificial Intelligence (AI) is "the study of ideas which enable computers to do things which make people seem intelligent" [WINSTON84]. AI encompasses a number of domains including natural language understanding, problem solving, game playing, robotics and vision. One of the "hottest" topics in AI today is the development of Expert Systems.

Rich states that an expert system is a set of programs that can perform an application such as medical diagnosis, electronic design and scientific analysis, that would normally be done by a human expert [RICH83]. The construction of such a system Rich calls Knowledge Engineering.

Basden states that expert systems are loosely defined as "computer systems that can hold human-like knowledge of (in theory) any kind and can process knowledge in a more human-like fashion that do conventional computer systems" [BASDEN84].

Goodall defines expert systems as "a computer system that operates by applying an inference mechanism to a body of specialist expertise represented in the form of 'knowledge'" [GOODALL85].

Coombs defines expert systems, as "automated knowledge-based problem solvers" [COOMBS84].

There are a wide variety of definitions of expert systems, depending on the authors point of view, and the literature contains discussions of various expert systems that span a wide range of task domains. Some of the more well known expert systems are given in table 1, along with other rule based systems that perform the function of image analysis and interpretation. These systems have different internal structures and computing mechanisms, however they all try to perform a function that could be done by a human. Many authors who develop complex systems based on AI techniques are reticent to call the systems expert, because they do not perform at the competence level of a human expert, often due of the complexity of the task. These systems have become known as rule-based systems or knowledge-based systems.

SYSTEM	PURPOSE	FUNCTION	AUTHORS
DENDRAL [LINDSAY80]	Generate plausible structural representations of organic molecules from mass spectrogram data	Data Interpretation	Feigenbaum, Lederberg
R1/XCON [MCDERMOTT82]	Configure Vax computers from customers orders	Design	McDermott
MYCIN [SHORTLIFFE76]	Diagnosis of bacterial infections and recommend antibiotic therapy	Diagnosis	Shortliffe
HEARSAY II [ERMAN80]	Speech understanding	Signal Interpretation	Erman, Lesser, Hayes-Roth, Reddy
PROSPECTOR [DUDA79]	Geological exploration	Data Interpretation	Duda, Hart
MAPS/SPAM [MCKEOWN85] [MCKEOWN84]	Map assisted photo interpretation	Image Analysis and Interpretation	McKeown, McDermott
MESSI [LEVINE86]	Image understanding	Image Analysis and Interpretation	Levine, Nazif
VISIONS [HANSON78]	Experimental environment for image interpretation system development	Image Analysis and Interpretation	Hanson, Riseman
ACRONYM [SHAPIRO85]	Precise photogrammetric image understanding	Image Analysis and Interpretation	Brooks, Binford, Bulloch
MICE [PLUNKETT86]	Map/image congruency evaluation	Image Analysis and Interpretation	Plunkett Goldberg Goodenough

MISSEE [GLICKSMAN82]	Image understanding using multiple information sources	Image Analysis and Interpretation	Glicksman Mackworth
ALVEN [TSOTSOS85]	Evaluation of heart motion using X-ray image sequences	Image Analysis and Interpretation	Tsotsos
ANGY [STANSFIELD86]	Automatic segmentation of coronary vessels	Image Analysis and Interpretation	Stansfield

Table 1 - Table Of Knowledge Based Systems

All expert systems have three common features. These are:

1. A human interaction capability
2. An inference engine
3. A knowledge base

The first common element of an expert system is the human-machine interaction capability, which is a mechanism that allows the human user to input information into the expert system and to obtain results. Expert system interaction then becomes a matter of translating the information that the human expert has provided into some form of knowledge representation for processing within the expert system. Output from an expert system may be in the form of speech, images or text. As with input, the output from an expert system ranges from the simple to the sophisticated, but output is essential for query and results presentation. The important factor here is that the human-machine interaction be syntactically and semantically correct for both the human and the expert system.

The second common element of an expert system is the inference engine. The inference engine organizes and controls the steps taken to solve the problem. One of the more common problem-solving paradigms involves the chaining of if-then rules to form a line of reasoning. If the

chaining starts from a set of conditions and moves to some conclusion or goal, then the method is called forward chaining. If the goal is known, but the path to the goal is not known, then working backwards from the goal in the search space, is called backward chaining.

Both forward and backward chaining through a large search space may cause a computational explosion. Appropriate domain heuristics or "rules of thumb" may be used to prune the search space, in order to achieve a more efficient expert system. Numerous search strategies such as depth first, breadth first, and A* search [WINSTON84] may be used in the inference engine in order to perform the search.

Meta reasoning may be used to decide what to do next. Meta rules from the knowledge base can be thought of as strategic or tactical layers in which, the inference engine decides among several possible strategies, what to do next. Meta rules may also be thought of as the procedural part of the expert system.

The third common element of an expert system is the knowledge base. This may be simply a store of domain rules used by the inference engine. The most popular approach to representing the domain knowledge is by production rules (also called condition-action rules or if-then rules). These rules may be specific domain knowledge coded as object rules or as meta rules. Many rule based systems

have a numerical certainty factor associated with each rule. These certainty factors are combined during the search procedure and are used to arrive at a certainty value for the final solutions.

The architecture and techniques employed in expert systems are varied and often complex. One approach to reducing the development cost of an expert system is to use a package called an expert system shell. A shell contains most of the elements of an expert system except the domain knowledge. The knowledge engineer can easily add rules to the knowledge base of the shell and thus develop an expert system more rapidly. Shells usually have additional elements to the three mentioned previously. These elements may include development and maintenance aids such as editors, file systems, debuggers, explanation facilities and traces.

Some of the more well known commercial shells are given in Table 2. [SCOWN85], [GEVARTNER82], [LETENDRE85].

Shell	Supplier	Description
Knowledge Craft	Carnegie Group, Inc.	An integrated knowledge Engineering and problem solving solving environment for building large expert systems.
ART - Automated Reasoning Tool	Inference Corporation	A generic problem solving paradigm including frames, rules, processes, common AI algorithms and data structures.
KEE - Knowledge Engineering Environment	IntelliCorp	A knowledge engineering environment incorporating frame-based and rule-based reasoning paradigms, knowledge manipulation, reasoning, and object oriented programming.
LOOPS	Xerox	A programming environment including procedure-oriented, object-oriented, data-oriented, and rule-oriented paradigms.
DUCK	Smart Systems Technology	A system builder including logic programming, rule-based reasoning, nonmonotonic reasoning, and deductive forward and backward search.
EXPERT-EASE	Jeffrey Perrone & Assoc.	A PC based expert system builder allowing the creation of models of expertise, that can be converted to inquiry systems.
S.1	Teknowledge, Inc.	A large scale software package allowing the experienced knowledge engineer to create practical applications.
TIMM	General Research Corp.	An expert system builder that uses a frame paradigm and a partial match analogical inferencing procedure that allows the use of incomplete or approximate knowledge.

EMYCIN	Stanford University	A skeleton expert system shell that was developed from MYCIN. EMYCIN uses backward-chaining control.
KAS	SRI International	A knowledge engineering tool that allows forward and backward chaining and a knowledge based editor. KAS was developed for use with the PROSPECTOR expert system.
ROSIE	Rand Corp	A general purpose rule based procedure-oriented system.

Table 2 - A List Of Commercial Expert System Shells.

4 THE MAP/IMAGE CONGRUENCY PROBLEM

For many years, human photo-interpreters have been analyzing air-photos, deciding on the classification of various objects in the photo and then transcribing the classification and location of these objects onto a map or more recently into a geographic information system [ZARZYKI82]. Since this map making procedure is primarily a human endeavor, it is prone to human error. In addition, the world land-mass is a constantly changing entity. For example, rivers meander, forests burn or are cut, and subdivisions and roads are built. Cartographic data on the other hand, is relatively static and is only updated periodically to reflect the changing world.

For some time, the remote sensing community has been extolling the virtues of the integration of remote sensing data with GIS data bases. This data integration problem has been researched and solutions developed, which are used operationally by some agencies [HEGYI83]. However, the automatic integration of remote sensing data with geographic information systems is not yet possible as it still requires human interpretation and assistance.

The integration problem occurs when an identified area in a remote sensing image, which is usually depicted as a polygon, is to be placed in a GIS. If the image polygon is placed directly into the GIS data base, then data base corruption will occur, if there is not perfect spatial

juxtaposition of the image polygon and the corresponding map polygon. The current method of performing this integration is for a human operator to move the image polygon into the best fitting location in the map and then place it in the GIS data base.

An example depicting the misregistration problem is given in Figures 1a and 1b. These Figures depict a Landsat MSS image overlayed with the hydrography level of a map. Figure 1a indicates the problem of image land pixels, that appear to be in the map river (Area A). Similarly, image river pixels that are outside the bounds of the map river (Area B) are indicated. Figure 1b indicates where the lake in the map appears to be in a slightly different location than the lake in the image (Area C).

Figure 1a - A Map/Image Overlay Depicting River Mismatch
This Landsat MSS image overlayed with the BC forest cover map (hydrology level) indicates the image land pixels that are in the river (Area A) and the image water pixels that are outside the map river (Area B).

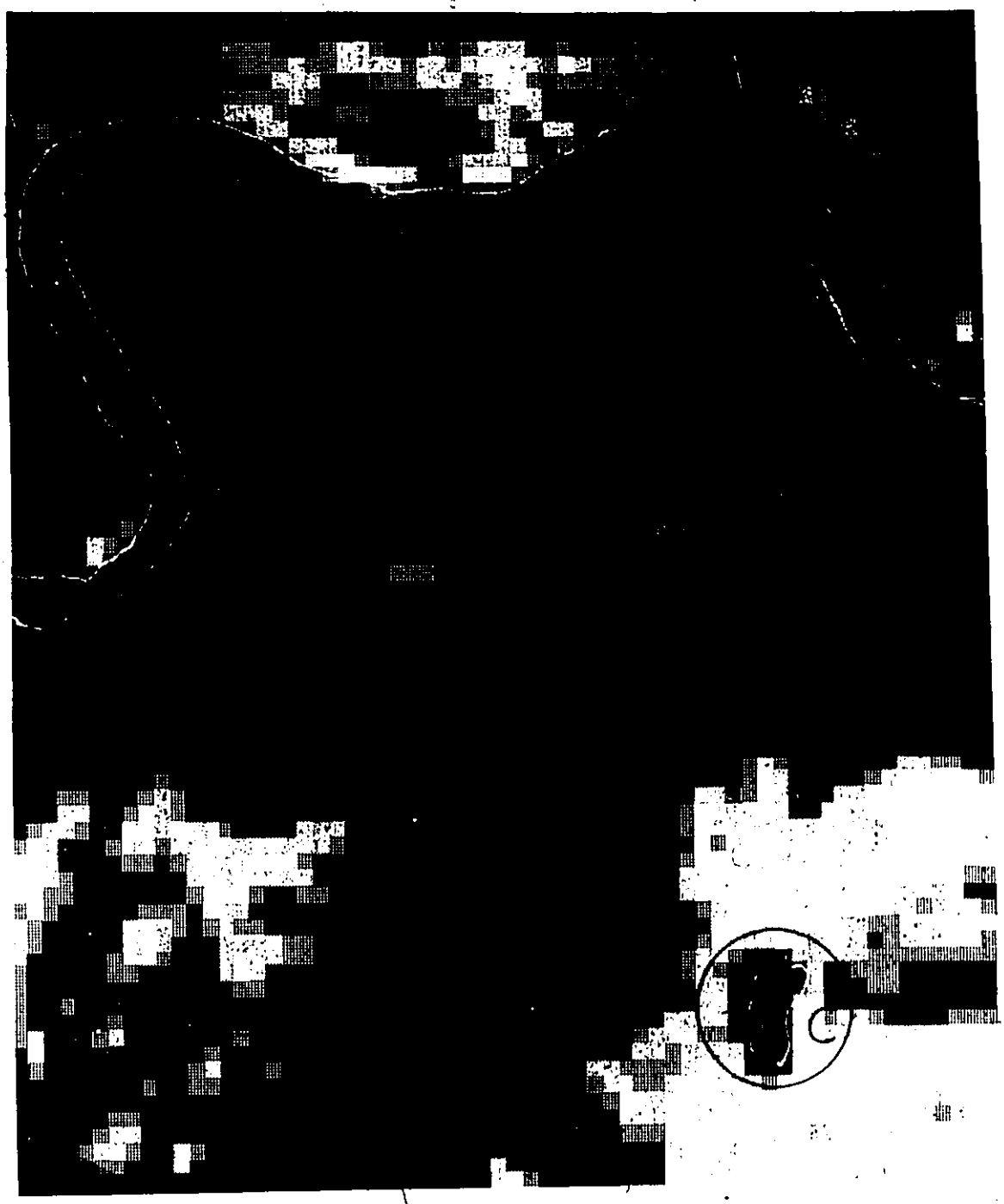

Figure 1b - A Map/Image Overlay Depicting Lake Mismatch

This Landsat MSS image overlayed with the BC forest cover map (hydrology level) indicates a spatial mismatch of the map lake and the image lake (Area C).

5 THE CONGRUENCY EVALUATION KBS DESIGN

Several design issues must be resolved before implementing the MICE KBS. These issues are:

1. How to uniformly represent the data?

2. What data attributes are required?

3. How is the coding to be implemented?

This section will discuss these design issues and present the selected solutions.

One of the first questions that must be answered in the design of the KBS is: how to represent these two disparate data types (ie map and image data) in a knowledge based system? Map data containing dots, lines and areas, is usually defined in a coordinate reference system in terms of points, vectors and polygons. Image data, on the other hand, is stored using a spatially indexed technique called raster or grid format. It would be extremely unwieldy to attempt to store and process this data in its native form in a knowledge based system, as the format, data type and resolution of the data are different. Also the system does not necessarily make decisions based on the data, but rather on various attributes derived from the data. Thus, the uniform data representation selected was to preprocess the map and image data into segments and to generate various symbolic segment attributes, that can then

be used by the rule-based stage.

The next question that needs to be answered then is: what attributes of the data are required for congruency evaluation? This question is also not easy to answer, because the image has spectral attributes that simply are not available in the map data. The image segments spectral attributes are required, so that the image segments can be spectrally classified. The map and image spatial attributes can be calculated relative to the same reference grid, so that the attribute values of the map and image can be compared in the KBS on an equivalent basis.

The spatial attributes selected for use by MICE, that are common to both the map and the image are as follows.

1. LOCATION - the location attribute represents the location of the pixels in the map or image segment, based on some reference grid. The value of the location attribute is a list of three-tuple lists that uniquely identify the location or position of the segment on a line by line basis. The three-tuple list contains:

    1. the line number containing the pixels.

    2. the start pixel number.

3. the end pixel number.

A list of these run length encoded three-tuples thus will define the location of the segment. A sample segment with its corresponding location attribute is depicted in Figure 2.

2. SIZE - the size attribute represents the size of the segment. The value of the size attribute is the total number of pixels in the segment. A sample segment with its corresponding size attribute is depicted in Figure 2.

3. SHAPE - the shape attribute represents the shape of the segment. The value of the shape attribute is the perimeter squared divided by the area. This shape attribute is a fairly primitive representation of the shape, but additional shape attributes can easily be added later. A sample segment with its corresponding shape attribute is depicted in Figure 2.

4. WINDOW - The window attribute represents the smallest rectangle that can be placed around the entire segment. The value of the window attribute is a list of four elements that represent the line and pixel locations of the upper left corner of the window, and the lower right corner. A sample segment with its corresponding window attribute is depicted in Figure 2.

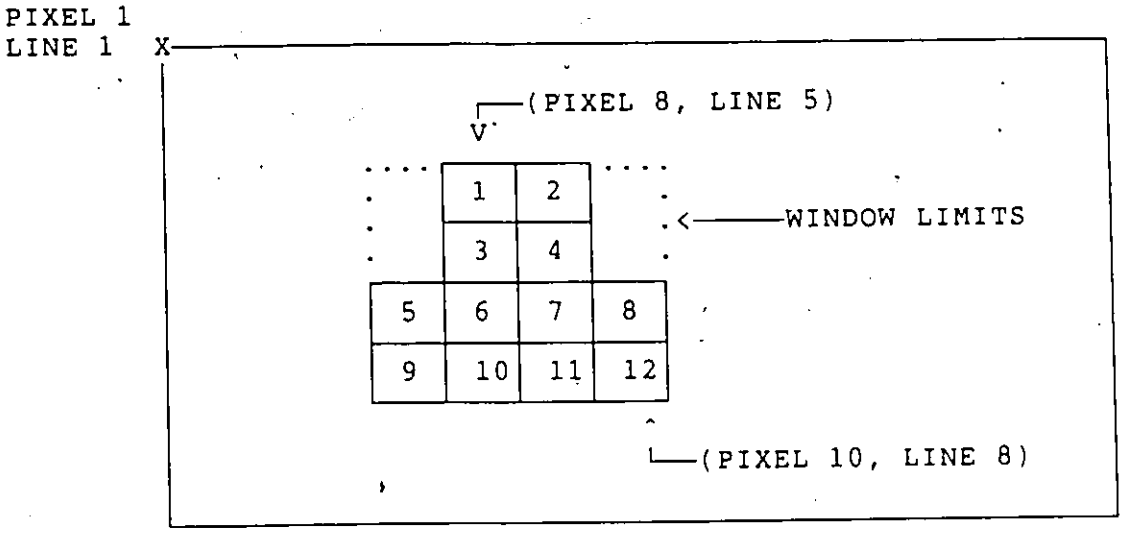


```
LOCATION = [[LINE, START PIX, END PIX]....]
         = [[5,8,9],[6,8,9],[7,7,10],[8,7,10]]

SHAPE    = (PERIMETER ** 2) / AREA
         = ((16 * 50) ** 2) / (50 * 50)
         = 256

SIZE     = PIXEL COUNT
         = 12

WINDOW   = [UPPER LEFT LINE, UPPER LEFT PIXEL,
            LOWER RIGHT LINE, LOWER RIGHT PIXEL]
         = [5, 7, 8, 10]
```

Figure 2 - The Spatial Attributes Of A Segment

The image spectral attributes that were selected for MICE processing are as follows:

1. MEAN_CH_1 - This attribute represents the mean grey level value of all the pixels in the segment for channel 1 (band 4, 0.5 to 0.6 micrometers wavelength, green spectral region) of the MSS

image.

2. MEAN_CH_2 - This attribute represents the mean grey level value of all the pixels in the segment for channel 2 (band 5, 0.6 to 0.7 micrometers wavelength, red spectral region) of the MSS image.

3. MEAN_CH_3 - This attribute represents the mean grey level value of all the pixels in the segment for channel 3 (band 6, 0.7 to 0.8 micrometers wavelength, near infrared spectral region) of the MSS image.

4. MEAN_CH_4 - This attribute represents the mean grey level value of all the pixels in the segment for channel 4 (band 7, 0.8 to 1.1 micrometers wavelength, near infrared spectral region) of the MSS image.

5. MAX_CH_1 - This attribute represents the maximum pixel grey level value in the segment for channel 1 of the MSS image.

6. MAX_CH_2 - This attribute represents the maximum pixel grey level value in the segment for channel 2 of the MSS image.

7. MAX_CH_3 - This attribute represents the maximum pixel grey level value in the segment for channel 3 of the MSS image.

8. MAX_CH_4 - This attribute represents the maximum pixel grey level value in the segment for channel 4 of the MSS image.

9. MIN_CH_1 - This attribute represents the minimum pixel grey level value in the segment for channel 1 of the MSS image.

10. MIN_CH_2 - This attribute represents the minimum pixel grey level value in the segment for channel 2 of the MSS image.

11. MIN_CH_3 - This attribute represents the minimum pixel grey level value in the segment for channel 3 of the MSS image.

12. MIN_CH_4 - This attribute represents the minimum pixel grey level value in the segment for channel 4 of the MSS image.

These spectral values may be used to evaluate the spectral classification of the segment corresponding to the attribute values. These spectral attributes are by no means an exhaustive list for classification determination, but they do provide a basis upon which other attributes can be added.

The final question that must be answered is: how to code the knowledge and make inferences on the attributes? One of the more cost effective methods of implementing a

knowledge based system is to use an already developed shell. MICE was designed to use the CCRS Remote Sensing Shell called RESHELL [GOLDBERG85], [BRAUN85]. RESHELL is a hierarchically designed system that is controlled by knowledge engineer supplied meta and object rules. RESHELL has many elements, but the most important ones for MICE are the data interface, the blackboard, the meta and object rule interpreters and the scheduler. More information on the internal structure of RESHELL is available in the references.

Following the preprocessing and congruency evaluation stage, a postprocessing stage was designed to convert the symbolic results files to imagery format for interpretation.

6 THE MICE KBS IMPLEMENTATION

6.1 THE PREPROCESSING STAGE

6.1.1 THE GIS PREPROCESSING STEPS -

The GIS preprocessing stage begins with the map data stored as an Intergraph design file. This file may contain a variety of cartographic information, but for the purposes of congruency evaluation, only certain cartographic features or levels may be required. It was found that on some levels, text was included as graphics within the level. If the text or symbols were left in, then as the level was rasterized and later input to the MICE KBS, the text would confuse the KBS, because the map data is classified by the level on which it appears in the file, thus text elements would not be properly classified. For instance if the text was left in the double line river level, then MICE would process this text as if it was a double line river, which it obviously is not. A method of circumventing this problem would be to develop a text and symbol recognition function in MICE, but this was deemed unnecessary at this time. The required levels are extracted and any spurious information or text is deleted. The levels are extracted into separate files, so that each level can be worked on individually.

Each level is then edited by a program, which uses an automated technique for ensuring that all line intersections were cartographically sound. This procedure ensures that there are no subtle faults in the vector data. The three basic faults that are corrected for, are normally expected in maps that have been hand digitized. These faults, which are depicted in Figure 3, are: 1) overshoot conditions; 2) undershoot conditions; and 3) knot conditions. All locations where these faults occur are identified, corrected, and a new map file created.

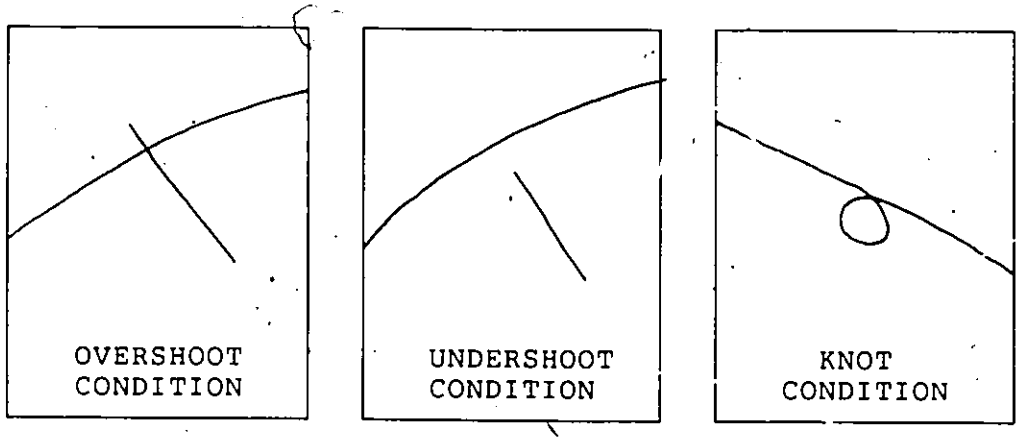

Figure 3 - Map Digitization Problems

Next, the levels are individually converted from vector format into grid format, based on a presence/absence algorithm. The presence/absence algorithm, which is depicted in Figure 4, simply determines if any part of a vector defined within the level touches anywhere within the grid square, if so, then the grid square is set to binary

1. Otherwise the grid square will be left as binary 0 (ie when no vector crosses it). The output of this process is a column major binary grid file. The grid spacing of 50 meters by 50 metres was selected as this is the grid spacing of the Landsat MSS geocoded product [GUERTIN81].

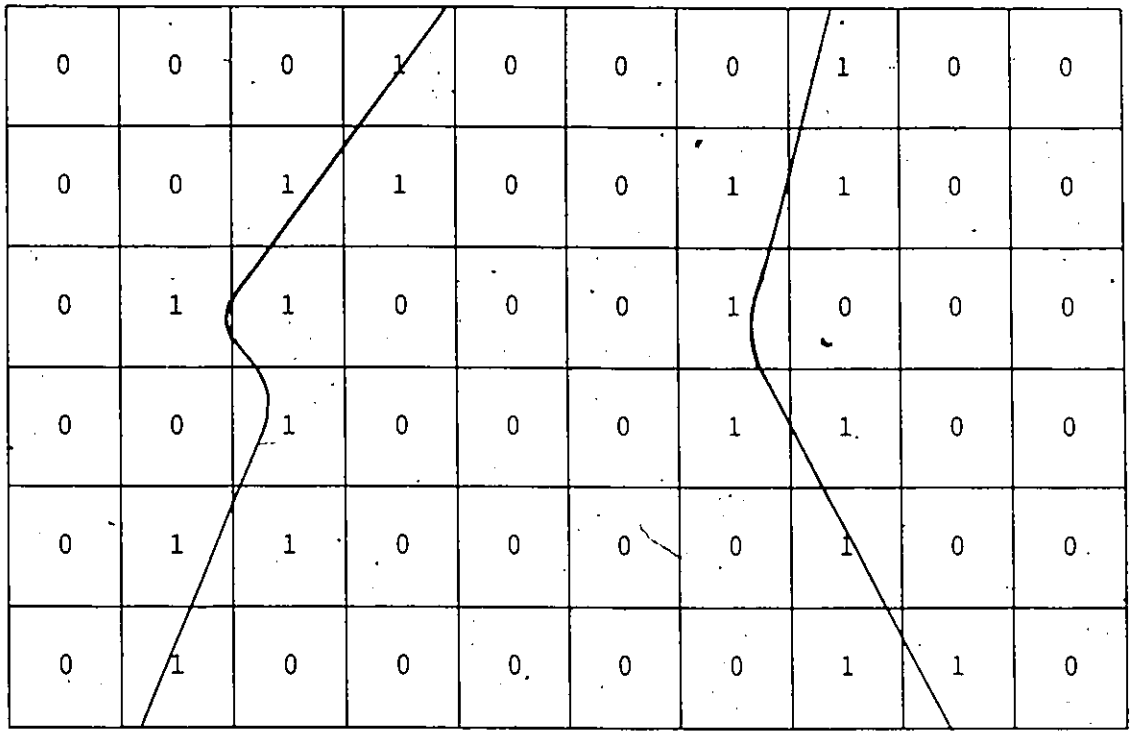

Figure 4. - The Presence Absence Algorithm

These grid files are then converted to CCRS standard imagery file format. This step converts the column major binary files into row major files, that are compatible with the remaining processes that are required. Each segment (such as a lake), which is not fully filled, is subsequently filled. Filling was found to be necessary for

further processing, as every map segment was to be handled as a polygon. Single line map elements like creeks are easily handled as polygons, as they are simply polygons with a width of one pixel.

The next stage is to precision register the raster map data with a UTM grid. This stage is very important as all spatial processing of the map data must be done with care or the evaluation of the congruency will give misleading results. This procedure consists of determining the exact UTM coordinates of a point in the image and the exact UTM coordinates of a point in the map. Then the map is translated to the proper position relative to the image. No scaling is required, since both the map and image are on a 50x50 meter grid. No rotation is required since both data sets are projected onto the same UTM grid.

The map data are then converted from the raster format file into a run-length encoded format file. This step saves much memory in the KBS as the map data is relatively sparse and thus all the run-length encoded positions of the map segments can easily be held in the KBS.

The final stage of processing is to convert the run-length encoded segment locations into symbolic format. The locations are defined in terms of object elements within the KBS. Thus there is one object element per map segment. Each map object element thus contains a location attribute and a list of the segment locations as the

attribute value. In addition, other segment attribute values such as size, shape and window are calculated at this time and placed in the attribute value positions of the symbolic object element. Also, context information about the object, such as: the segment number, the source of the segment and the map classification of the segment are included.

The procedure for preprocessing the cartographic data is given in Figure 5. These map preprocessing steps are currently requested manually, but there is no reason why some of these map preprocessing stages could not be added to the rule-based stage, so that they could be run more autonomously of the user.

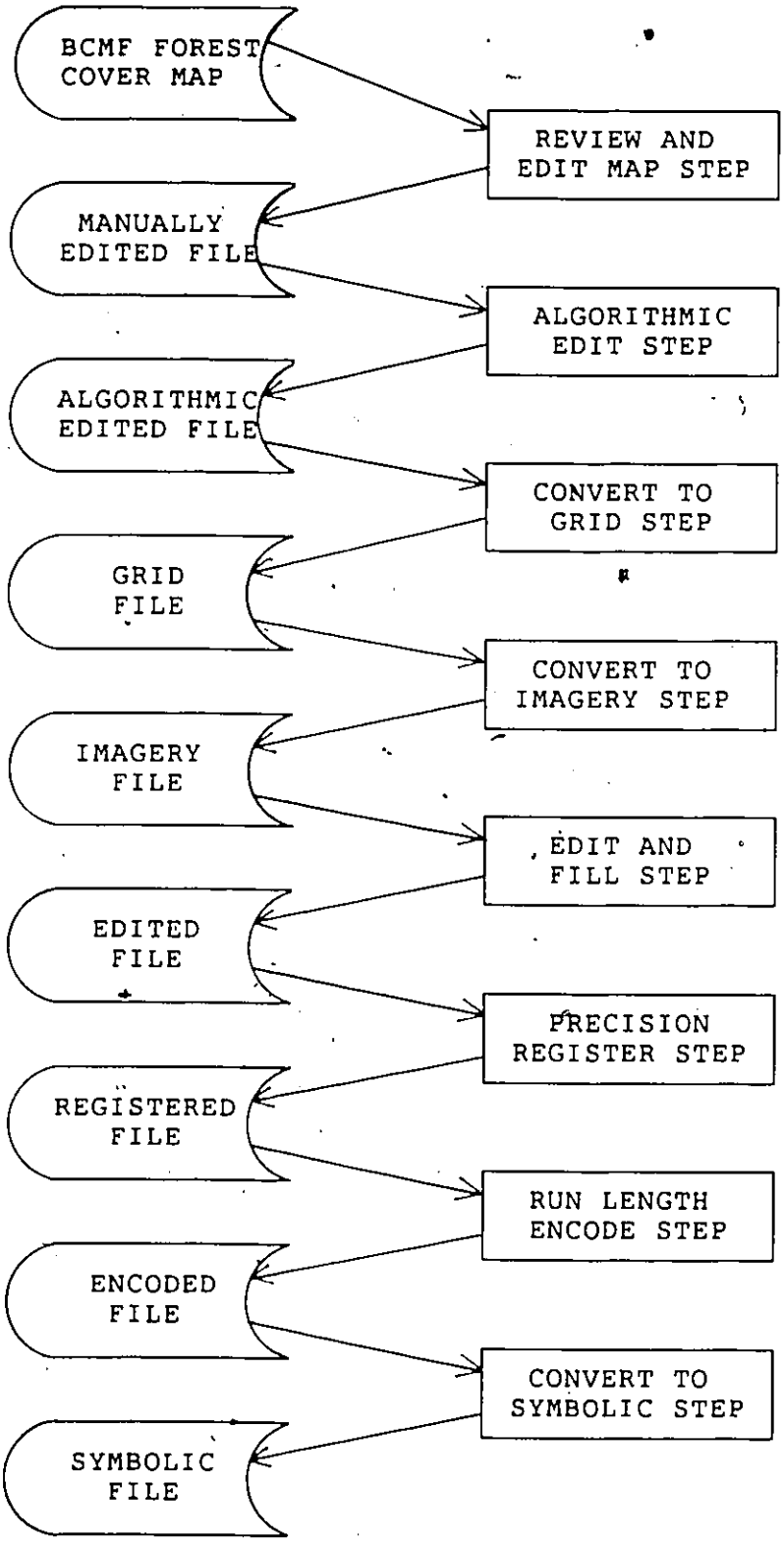

Figure 5 - Map Preprocessing Stage

6.1.2. THE IMAGE PREPROCESSING STEPS -

The image preprocessing stage begins with the extraction of the sub-area of the geocoded MSS image that corresponds to the the map. This image file is then operated on by a gradient operator, and segmented [BEAULIEU85]. The Sobel gradient operator has given the best results to date. The segmentation operator generates a large number of segments from the gradient image and these are then run-length encoded. The image spatial attributes are then converted to a symbolic file. The original sub-image and the segment location file are then input to a program, which generates a segment spectral statistics file. This file is then converted to symbolic form. The resulting symbolic image locations file and symbolic image statistical file are then available for input to the MICE KBS. The preprocessing steps for the geocoded MSS data is given in Figure 6.

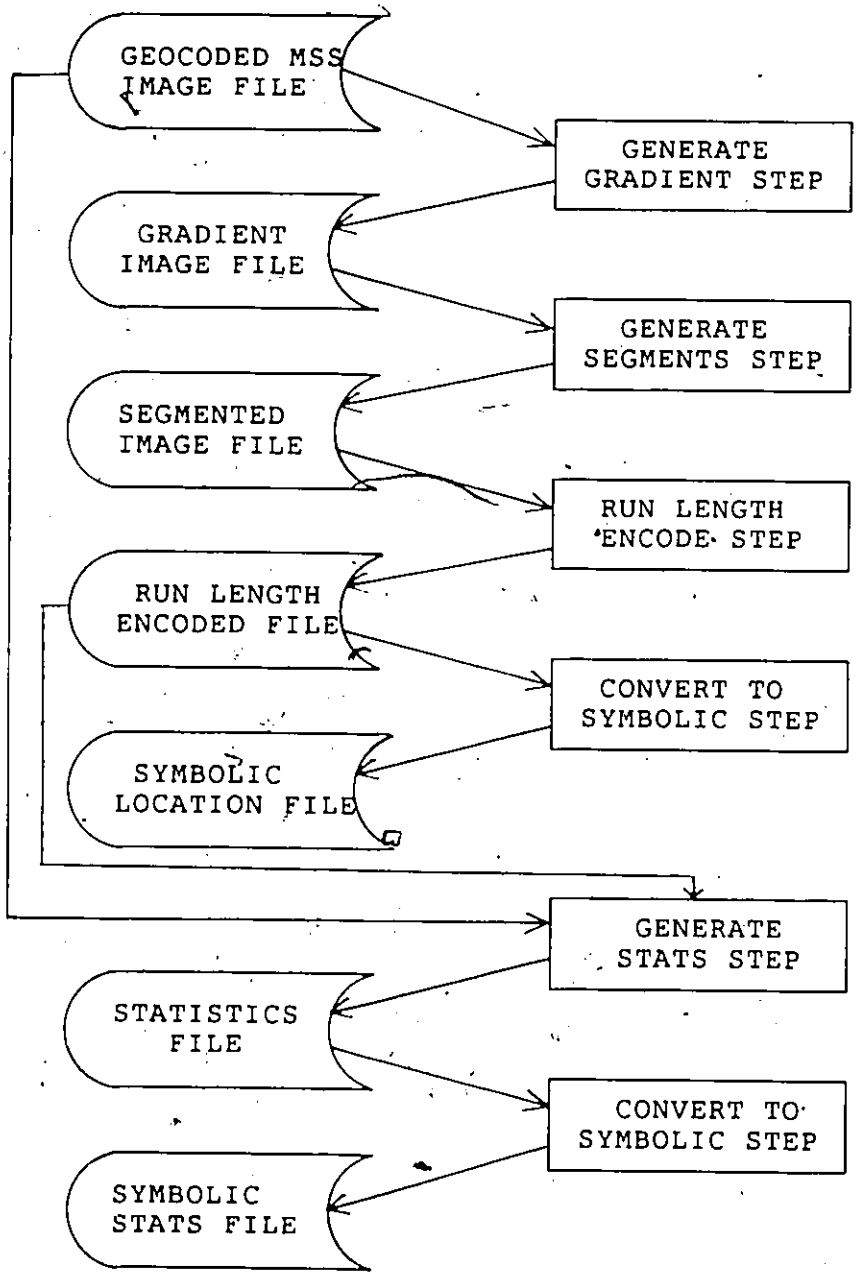

Figure 6 - MSS Image Preprocessing Stage

6.2 THE RULE-BASED STAGE

The basic elements of the rule-based stage are depicted in Figure 7 and are as follows:

1. map segments location symbolic file
2. image segments location symbolic file
3. image segments statistics symbolic file
4. inference engine
5. knowledge base
6. terminal input/output
7. congruency results symbolic file

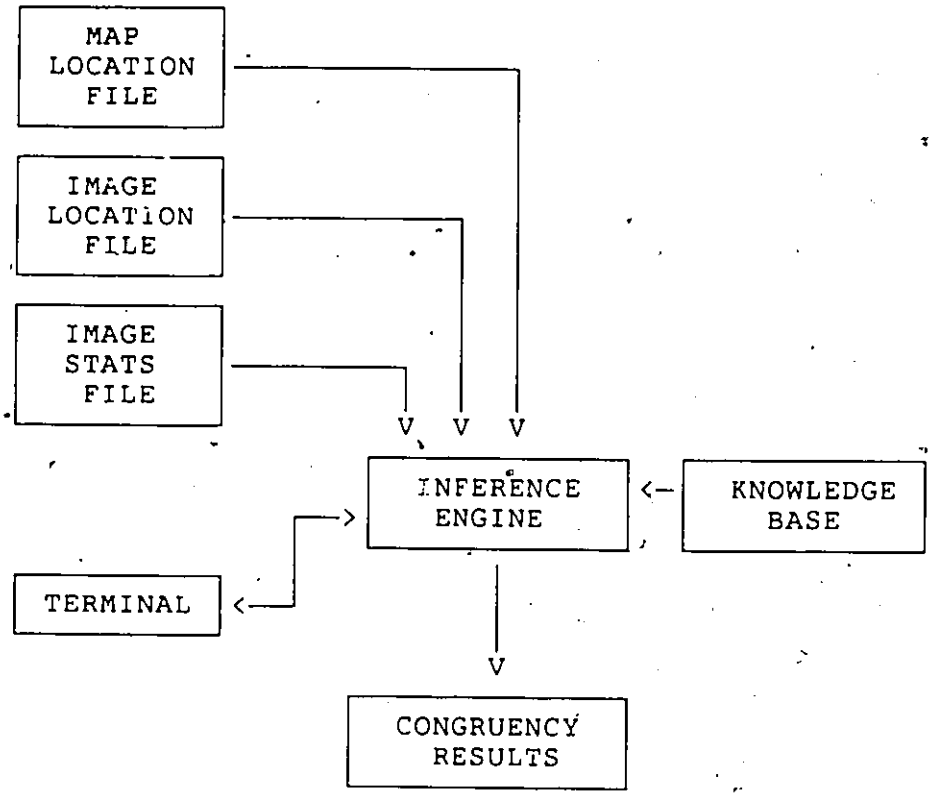

Figure 7 - The Elements Of The Rule-Based Stage

6.2.1 THE MAP SEGMENTS LOCATION SYMBOLIC FILE -

The map segments location symbolic file is generated by the map preprocessing stages that were described earlier. In order to speed the reading of the map information into the rule-based stage, the object attributes are coded into one record, which is split up by MICE after input, into the individual object-attribute-value combinations. The format of the object attributes in the symbolic map segments location file is as follows, in Prolog notation:

```
obj([[*,source(map_bcfs),*,segment(segment#),
      *,class(map_class),*],
location,
[
[line#n,   start_pixel_line#n,
       stop_pixel_line#n  ],
[line#n+1, start_pixel_line#n+1,
       stop_pixel_line#n+1],
.
.
.
[line#n+m, start_pixel_line#n+m,
       stop_pixel_line#n+m]
],
size,
[segment_size],
shape_1,
[
segment_shape
],
window,
[upper_left_pixel, upper_left_line,
        lower_right_pixel, lower_right_line],
[measure_of_belief, measure_of_disbelief],
]).
```

The meaning of the various attributes and values was given in Figure 2. The rule-based stage inputs this record and then stores the 4 attributes (location, size, shape,

and window) as separate attribute-value combinations in the data base partition of the MICE blackboard. For example, a sample input entity might look as follows:

```
obj([ [*,source(map_bcfs),*,segment(205),
                *,class(hydrography),*],
location, [ [148,274,275],[149,274,275] ],
size,     [4],
shape_1,  [ 0.1600E+02 ],
window,   [148,274,149,275],
[75,0] ]).
```

After the record is read, the following object values for each attribute are stored in the blackboard. Note that the object context-attribute-value tuples are now separated out, where in the previous record, there was only one context value for all the attributes.

```
obj([ [*,source(map_bcfs),*,segment(205),
                *,class(hydrography),*],
location, [ [148,274,275],[149,274,275] ],
[75,0]]).

obj([ [*,source(map_bcfs),*,segment(205),
                *,class(hydrography),*],
size, [4],
[75,0]]).

obj([ [*,source(map_bcfs),*,segment(205),
                *,class(hydrography),*],
shape_1, [ 0.1600E+02 ],
[75,0]]).

obj([ [*,source(map_bcfs),*,segment(205),
                *,class(hydrography),*],
window, [148,274,149,275],
[75,0]]).
```

6.2.2 THE IMAGE SEGMENTS LOCATION SYMBOLIC FILE

The image segments location symbolic file is generated by the image preprocessing stage that was described in Figure 6. In order to speed the reading of the image information into the rule-based stage, the object attributes are coded into one record, using the same principle as for the map segments location file. The format of the object attributes in the symbolic map segments locations file is as follows, in Prolog notation:

```
obj([
[*,source(image_mss),*,segment(segment#),
                              *,class(unknown),*],
location,
[
[line#n,    start_pixel_line#n,
                    stop_pixel_line#n  ],
[line#n+1, start_pixel_line#n+1,
                    stop_pixel_line#n+1],
.
.
.
[line#n+m, start_pixel_line#n+m,
                    stop_pixel_line#n+m]
],
size,
[segment_size],
shape_1,
[
segment_shape
],
window,
[upper_left_pixel, upper_left_line,
      lower_right_pixel, lower_right_line],
[measure_of_belief, measure_of_disbelief],
]).
```

Following the reading of this segment location record and the reading of the corresponding segment statistics record, MICE decides on a classification for the segment. This class value is then stored in the context portion of

the object. For example, if the segment was classified as hydrography, then the context portion becomes:

```
obj([
[*,source(image_mss),*,segment(205),
                    *,class(hydrography),*],
location,
[
[148,274,275],[149,274,275]
],
[75,0]
]).
```

6.2.3 THE IMAGE SEGMENTS STATISTICS SYMBOLIC FILE -

The image segments statistics symbolic file is generated by the image preprocessing stage described previously and depicted in Figure 6. The format of the object attributes in the symbolic image statistics file is as follows, in PROLOG notation:

```
obj([
[*,source(image_mss),*,segment(segment#),
                          *,class(unknown),*],
size,
[segment_size],
MEAN_CH_1,
[channel_1_mean_value],
mean_ch_2,
[channel_2_mean_value],
mean_ch_3,
[channel_3_1_mean_value],
mean_ch_4,
[channel_4_mean_value],
max_ch_1,
[maximum_pixel_value_in_channel_1],
max_ch_2,
[maximum_pixel_value_in_channel_2],
max_ch_3,
[maximum_pixel_value_in_channel_3],
max_ch_4,
[maximum_pixel_value_in_channel_4],
min_ch_1,
[minimum_pixel_value_in_channel_1],
min_ch_2,
[minimum_pixel_value_in_channel_2],
min_ch_3,
[minimum_pixel_value_in_channel_3],
min_ch_4,
[minimum_pixel_value_in_channel_4],
[measure_of_belief, measure_of_disbelief],
]).
```

The meaning of the various attributes was given in the previous section. The rule-based stage reads this object record and by evaluating the values of the channel means, decides on the class of the segment. Once the class is

determined, the name of the class is placed in the class portion of the rule context, replacing the value "unknown". This class name is added to the context or description field of all the location attributes for size, shape, location and window. The segment spectral attributes are not currently stored in the blackboard, as they are not used, once the class of the segment has been determined. If the spectral attributes were required, then the commands to store the attributes in the blackboard could be easily added. However, in the current implementation, the segment spectral attributes are not retained, in order to save on storage space.

6.2.4 THE INFERENCE ENGINE -

The inference engine is the part of the MICE KBS that performs the deductive reasoning, based on the rules in the knowledge base. The MICE KBS inference engine is provided by the CCRS remote sensing expert shell (RESHELL). RESHELL allows a hierarchical structure of "experts" that perform specific tasks based on the knowledge provided for that "expert". The architecture of the MICE KBS is depicted in Figure 8.

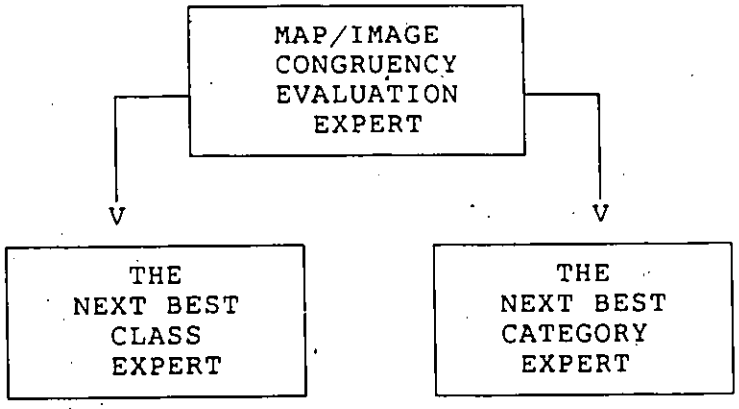

Figure 8 - Hierarchical Organization Of The MICE KBS

The generic architecture of an individual expert module is depicted in Figure 9.

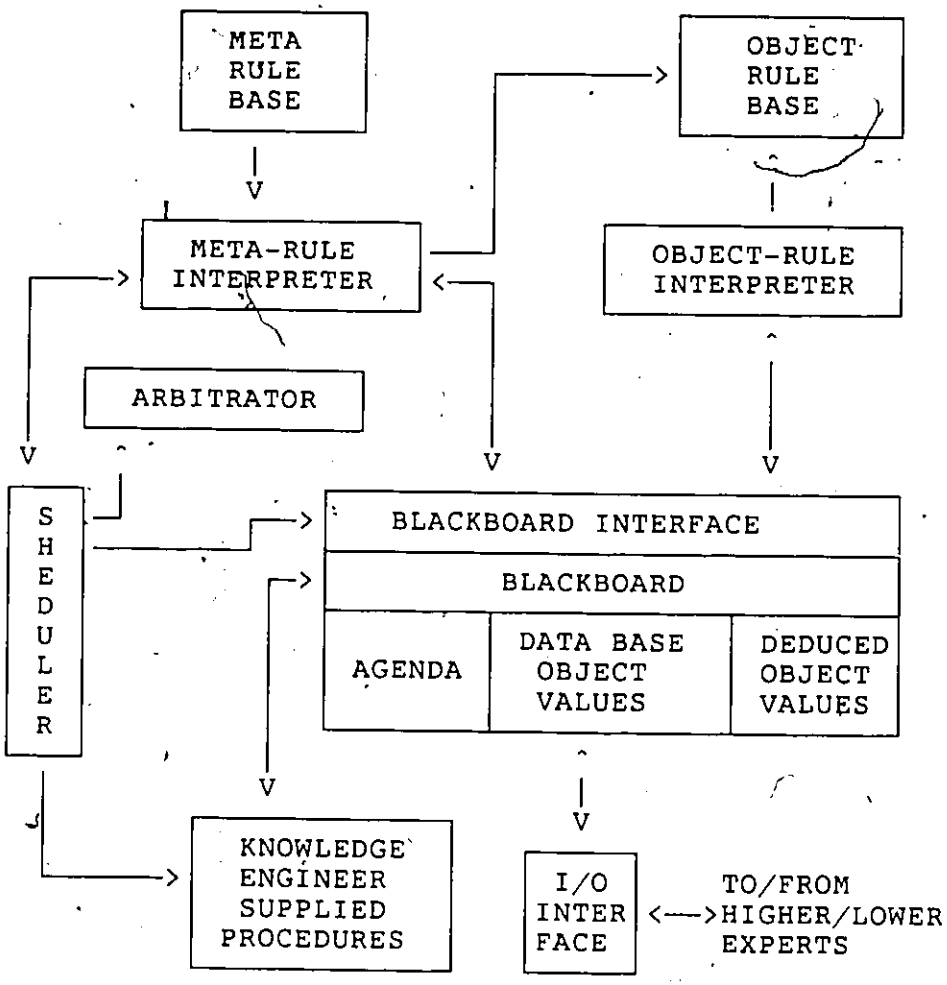

Figure 9 - The Architecture Of An Individual MICE "Expert"

The instantiations of RESHELL that perform the tasks of determining the next best class and the next best category are very straight forward and do not have much "expert specific" PROLOG code in the knowledge engineer supplied procedures part of the shell. However the main portion of the MICE KBS has a great deal of expert specific PROLOG code in the knowledge engineer supplied procedures section of the shell. This PROLOG code performs tasks that are requested by firing of meta-level rules from the knowledge base.

The main PROLOG predicates that are currently coded into the knowledge engineer supplied procedures section of the MICE KBS, correspond to the following meta-level rules:

1. load_the_map_segment_data_from_the_file (FILE_NAME) - This predicate loads the symbolic map locations data from the specified file into the database partition of the blackboard.

2. map_segments_file_loaded (OK) - This predicate ensures that there were no errors during the loading of the symbolic map data.

3. load_the_image_segment_data_from_the_files (TRU_FILE, STI_FILE) - This predicate loads the symbolic image locations file, the symbolic image statistics file, classifies the segments and stores the necessary information in the database partition of the blackboard.

4. image_segments_file_loaded (OK) - This predicate ensures that there were no errors during the loading of the image locations and statistics files.

5. the_current_class_is (CLASS) - This predicate retrieves the current class value from the database partition of the blackboard.

6. the_current_category_is (CATEGORY) - This predicate retrieves the current category value from the database partition of the blackboard.

7. the_next_best_class_is (CLASS) - This predicate retrieves the next best class value from the database partition of the blackboard.

8. start_get_the_next_best_class_expert (CURRENT_CLASS, CURRENT_CATEGORY, NEXT_CLASS) - This predicate initializes and starts the next best class sub-expert.

9. get_the_next_best_class (CURRENT_CLASS, NEXT_CLASS) - This predicate cleans up after calling the next best class expert and stores the next class value in the database partition of the blackboard.

10. calculate_map_area_for_class (CLASS, AREA) - This predicate calculates the total area of class (CLASS) from the map locations data.

11. calculate_image_area_for_class (CLASS, AREA) - This predicate calculates the total area of class (CLASS) from the image locations data.

12. the_size_difference_is_greater_than (THRESHOLD) - This predicate compares the subtracts the total image class area from the total map class area and returns false if the difference is larger than the threshold.

13. start_get_the_next_best_category_expert (CURRENT_CLASS, CURRENT_CATEGORY, NEXT_CATEGORY) - This predicate initializes and starts the next best category sub-expert.

14. get_the_next_best_category (CURRENT_CATEGORY, NEXT_CATEGORY) - This predicate cleans up after calling the next best category expert and stores the next category value in the database partition of the blackboard.

15. the_next_category_of_class_is (CLASS, CATEGORY) - This predicate retrieves the next category value from the database partition of the blackboard.

16. get_the_next_map_segment_of (CATEGORY, SEGMENT) - This predicate retrieves the next largest map segment from the sorted list of loaded map segments.

17. the_next_map_segment_of_category__is (CATEGORY, SEGMENT) - This predicate retrieves the next map segment of the specified category from the database partition of the blackboard.

18. get_all_image_segments_in_map_window (IMG_SEG_LIS) - This predicate returns a list of all the image segments that were deemed to be within the window of current map segment.

19. image_window_segments_is (SEGLIS) - This predicate retrieves the list of the image segments within the map window, from the database partition of the blackboard.

20. mark_results (FILEO_NAME, CLASS, ATTR) - This predicate outputs the symbolic locations information of the image segments that were determined to match the specified attribute.

21. compare_map_and_image_segment_classes - This predicate compares the class value in the context part of the map and image objects and stores a list of the matching image segments in the blackboard.

22. image_segments_identified (OK) - This predicate checks to ensure that there were no errors during the comparison of the segment classes.

23. compare_map_and_image_segment_sizes - This predicate compares the size attribute values of the map and image objects and stores a list of the segments that meet the following matching criteria in the blackboard. The matching size criteria is that the ratio of the map to image size be larger that .5 but less than 1.5.

24. segment_sizes (OK) - This predicate checks to ensure that there were no errors during the evaluation of the matching of the segments of similar size.

25. compare_map_and_image_segment_shapes - This predicate compares the shape attribute values of the map and image objects and stores a list of the segments that meet the following matching criteria in the blackboard. The matching shape criteria is that the ratio of the map to image shape be larger that .5 but less than 1.5.

26. segment_shapes (OK) - This predicate checks to ensure that there were no errors during the evaluation of the matching of the segments of similar shape.

27. compare_map_and_image_segment_locations - This predicate compares the locations attribute values of the map and image objects and stores a list of the segments that have overlapping locations in the blackboard.

28. segment_locations_match (OK) - This predicate checks to ensure that there were no errors during the evaluation of the matching of the segments with overlapping locations.

The inference engine used for the MICE KBS is thus provided by the RESHELL shell, however a significant portion of code was required to perform some of the special operations that are required for congruency evaluation.

6.2.5 THE KNOWLEDGE BASE -

Knowledge for the MICE KBS is coded in the form of meta-rules, object-rules, and object values. The rules and values are stored in a knowledge base file that is read in when an instantiated RESHELL expert is invoked. The MICE KBS uses only meta-rules and object-rules. There are no object values input from the knowledge base. The object values required for MICE processing are read in from the symbolic map and image files, as discussed earlier.

A meta-rule is coded in the following format:

```
mknb( [list of actions],
      [list of conditions],
      phase number,
      rule number ).
```

The meta-rule interpreter examines the list of conditions and if all of the conditions are determined to be true, then the list of actions is performed. Obviously, if any one of the list of conditions is not true, then no actions are performed. The phase number corresponds to the steps or stages in the agenda. The rule number is used to uniquely identify each rule.

An object-rule is coded in the following format:

```
knb( [list of actions],
     [list of conditions],
```

[certainty factor],
rule number).

The list of conditions is evaluated by the object level interpreter and if they are all successful, then the list of actions is performed. The certainty factor gives the measure of belief and the measure of disbelief for this rule and the rule number uniquely identifies each object rule.

One of the major advantages of the RESHELL architecture is that an instantiated expert does not have access to the rules in another instantiated expert's knowledge base. Thus, each of the three MICE experts (see figure 8) have separate and distinct rule codified knowledge. The rules for each expert will now be discussed.

6.2.5.1 **THE MICE EXPERT KNOWLEDGE BASE** -

The rules stored in the MICE expert knowledge base are meta-rules that define the strategy to be applied to the map/image congruency evaluation problem. The strategy or procedure is depicted as follows:

```
mknb([ nl,write(" Start of The MICE SYSTEM "),nl,
       load_the_map_segment_data_from_the_file
                              ("eskbs:maptru.sym") ],
     [ the_command_from_the_parent_expert_is
                              (run_mice) ],
     1 , 1 ).

mknb([ load_the_image_segment_data_from_the_files
       ("eskbs:imatru.sym", "eskbs:imasti.sym") ],
     [ map_segments_file_loaded(ok) ],
     2 , 2 ).

mknb([ write_the_string
          (" error loading map segments file"),
       del_mrules(4,25),
       return_final_results_to_parent_expert ],
     [ not(map_segments_file_loaded(ok)) ],
     2 , 3 ).

mknb([ start_get_the_first_best_class_expert
       (CUR_CLASS,CUR_CATEGORY,NEXT_CLASS),
       get_the_next_best_class
```

```
        (CUR_CLASS,NEXT_CLASS) ],
      [ image_segments_file_loaded(ok),
        the_current_class_is(start),
        the_current_category_is(start) ],
        3 , 4 ).

mknb([ start_get_the_next_best_class_expert
        (CUR_CLASS,CUR_CATEGORY,NEXT_CLASS),
        get_the_next_best_class
        (CUR_CLASS,NEXT_CLASS) ],
      [ image_segments_file_loaded(ok),
        not(the_current_class_is(done)),
        the_current_category_is(done) ],
        3 , 5 ).

mknb([ write_the_string
         (" error loading image segments file"),
        del_mrules(6,25),
        return_final_results_to_parent_expert ],
      [ not(image_segments_file_loaded(ok)) ],
      3 , 6 ).

mknb([ write_the_string(" all classes done"),
        del_mrules(8,25),
        return_final_results_to_parent_expert ],
      [ the_next_best_class_is(CLASS),
        the_is_equal_to(CLASS,done) ],
      4 , 7 ).
```

```
mknb([ calculate_map_area_for_class(CLASS,AREA),
       calculate_image_area_for_class(CLASS,AREA) ],
     [ the_next_best_class_is(CLASS),
       not(the__is_equal_to(CLASS,done)) ],
     4 , 8 ).

mknb([ start_get_the_next_best_category_expert(
          CUR_CLASS,CUR_CATEGORY,NEXT_CLASS),
       get_the_next_best_category
          (CUR_CATEGORY,NEXT_CATEGORY) ],
     [ not(the_size_difference_is_greater_than(100)),
       the_current_category_is(CUR_CATEGORY),
       not(the__is_equal_to(CUR_CATEGORY,done)),
       not(the_current_class_is(done)) ],
     5 , 9 ).


mknb([ start_get_the_next_best_category_expert(
          CUR_CLASS,CUR_CATEGORY,NEXT_CLASS),
       get_the_next_best_category
          (CUR_CATEGORY,NEXT_CATEGORY) ],
     [ the_size_difference_is_greater_than(100),
       the_answer_to__is
          ("large difference - proceed anyway ?",yes),
       the_current_category_is(CUR_CATEGORY),
       not(the__is_equal_to(CUR_CATEGORY,done)),
       not(the_current_class_is(done)) ],
     5 , 10 ).
```

```
mknb([ write_the_string
        (" Returning To Parent Expert "),
       del_mrules(11,25),
       return_final_results_to_parent_expert ],
     [ the_size_difference_is_greater_than(100),
       the_answer_to__is
        ("large difference - proceed anyway ?",no) ],
     5 , 11 ).

mknb([ restore_mrules(4,13) ],
     [ the_next_category_of_class__is(CLASS,CATEGORY),
       the__is_equal_to(CATEGORY,done)  ],
     6 , 12 ).

mknb([ get_the_next_map_segment_of(CATEGORY,SEGMENT) ],
     [ the_next_category_of_class__is(CLASS,CATEGORY),
       not(the__is_equal_to(CATEGORY,done)) ],
     6 , 13 ).


mknb([ restore_mrules(9,15) ],
     [ the_next_map_segment_of_category__is
        (CATEGORY,SEGMENT),
       the__is_equal_to(SEGMENT,done) ],
     7 , 14 ).

mknb([ get_all_image_segments_in_map_window(SEGLIS) ],
     [ the_next_map_segment_of_category__is
```

```
        (CATEGORY,SEGMENT),
        not(the__is_equal_to(SEGMENT,done)) ],
      7 , 15 ).

mknb([ restore_mrules(12,17) ],
     [ image_window_segments_is(SEGLIS),
       the__is_equal_to(SEGLIS,done) ],
     8 , 16 ).

mknb([ compare_map_and_image_segment_classes ],
     [ image_window_segments_is(SEGLIS),
       not(the__is_equal_to(SEGLIS,done)) ],
     8 , 17 ).

mknb([ mark_results
       ("eskbs:clas.res",hydrography,imgclaslis),
       compare_map_and_image_segment_sizes ],
     [ image_segments_identified(ok) ],
     9 , 18 ).

mknb([ write_the_string("no image class segments"),
       restore_mrules(12,19) ],
     [ image_segments_identified(done) ],
     9 , 19 ).

mknb([ mark_results
       ("eskbs:size.res",hydrography,imgsizlis),
       compare_map_and_image_segment_shapes ],
     [ segment_sizes(ok) ],
     10 , 20 ).
```

```
mknb([ write_the_string("no size difference"),
       restore_mrules(12,21) ],
     [ segment_sizes(done) ],
     10 , 21 ).

mknb([ mark_results
       ("eskbs:shap.res",hydrography,imgshaplis),
       compare_map_and_image_segment_locations ],
     [ segment_shapes(ok) ],
     11 , 22 ).

mknb([ write_the_string
       ("no segment size differences"),
       restore_mrules(12,23) ],
     [ segment_shapes(done) ],
     11 , 23 ).

mknb([ mark_results
       ("eskbs:over.res",hydrography,imgovrlis),
       restore_mrules(12,25) ],
     [ segment_locations_match(ok) ],
     12 , 24 ).

mknb([ write_the_string("no location differences"),
       restore_mrules(12,25) ],
     [ segment_locations_match(done) ],
     12 , 25 ).
```

6.2.5.2 **THE BEST CLASS EXPERT KNOWLEDGE BASE** -

The rules stored in the best class expert knowledge base are meta rules and object rules that define the order of classes from which to select segments for congruency evaluation. The classes that are currently defined were selected from the Canada Council on Surveys and Mapping [ZARZYKI82] list of classes and are ranked for congruency evaluation as follows:

CLASS CODE	CLASS DESCRIPTION	RANKING
G	Hydrography	1
D	Road and Rail	2
E	Utility	3
I	Land Cover	4
H	Hypsography	5
C	Structures	6
B	Buildings	7
A	Designated Areas	8
F	Delimiters	9
J	Text	10

Table 3 - Class Ranking For Congruency Evaluation

This table is coded into the form of object rules. For example, if the current class is Hydrography, then the next best class is Road and Rail. This knowledge is codified by the following rule:

```
knb([ obj([[*,class(hydrography),*,other(data),*],
```

```
                next_best_class, road_and_rail]) ],
    [ obj([[*,class(hydrography),*,other(data),*],
                class,X]) ],
    100, 2 ).
```

The best class expert selects the next best class by the rankings of Table 3 and passes this class information back to the MICE expert when requested.

6.2.5.3 THE BEST CATEGORY EXPERT KNOWLEDGE BASE -

Like the best class expert, the best category expert contains meta and object rules that define the next best category, based on the current class and category. The categories list also is derived from the Canada Council on Surveys and Mapping list of categories of classes. The categories of the various classes are ranked as follows for congruency evaluation.

CLASS	CATEGORY	RANKING
HYDROGRAPHY	COASTAL FEATURE	1
	INLAND WATER BODY	2
	WATER COURSE ASSCOC FEATURE	3
	GROUND WATER FEATURE	4
	WETLANDS	5
	RELATED HYDROGRAPHIC FEATURE	6
	PERMANENTLY FROZEN FEATURE	7
ROAD AND RAIL	ROADWAY	1
	THROUGH RAIL LINE	2
UTILITY	UTILITY	1
LAND COVER	WOODLAND	1
	ARABLE CULTIVATED LAND	2
	GRASSLAND	3
	LOW VEGETATION	4
	NO VEGETATION	5
HYPSOGRAPHY	HYPSOGRAPHY	1
STRUCTURES	STRUCTURES	1

BUILDINGS	BUILDINGS	1
DESIGNATED AREAS	DESIGNATED AREAS	1
DELIMITERS	DELIMITERS	1
TEXT	TEXT	1

Table 4 - Class Category Ranking For Congruency Evaluation

This category table is coded into the form of object rules and is evaluated by the category expert when requested, and the next best category (by ranking) is passed back following evaluation. A sample object rule from the next best category is as follows:

```
knb([ obj([[*,category(grassland),*,other(data),*],
        next_best_category, low_vegetation]) ],
      obj([[*,class(land_cover),*,other(data),*],
        class, X ]),
      obj([[*,category(grassland),*,other(data),*],
        category, Y ] ],
      100,17).
```

This rule codifies the knowledge that if the current class is Land_cover and the current category is Grassland, then the next best category is Low_vegetation.

6.2.6 THE TERMINAL I/O -

At the moment there is little information requested from the user by the MICE KBS. The major decision point, where the user is asked to proceed or to stop processing occurs when the MICE KBS determines that there is a substantial difference in the area of the current class in the map as compared to the image class area. This prompt allows the user to stop and check to ensure that he has the correct files.

MICE outputs information that is being used in the congruency evaluation processing and progress information is output at appropriate times. An example of the MICE terminal output is given in the sample run section.

6.2.7 THE CONGRUENCY RESULTS SYMBOLIC FILE -

The results of the congruency analysis are output to a symbolic results file, that can be converted to image format during the postprocessing stage. The format of the object elements in the results file are as follows:

```
obj([
[*,source(mice_kbs),*,segment(segment#),
      *,class(class),*],
location,
[[line,start_pixel,end_pixel],

 [end_line,start_pixel,end_pixel]],
[measure of belief, measure of disbelief] ]).
```

A sample results object element is as follows:

```
obj([
[*,source(mice_kbs),*,segment(20),
        *,class(hydrography),*],
location,
[[10,10,20],[11,10,20],[12,15,18]],
[100,0] ]).
```

6.3 THE POSTPROCESSING STAGE

Following the execution of the MICE KBS rule-based stage, the first step of the post-processing stage is to convert the symbolic results files to run-length encoded format. Following this step, a program is executed to convert the run-length encoded file into an image format file. This image may be qualitatively evaluated or statistical information on the various classes may be gathered for quantitative congruency evaluation information.

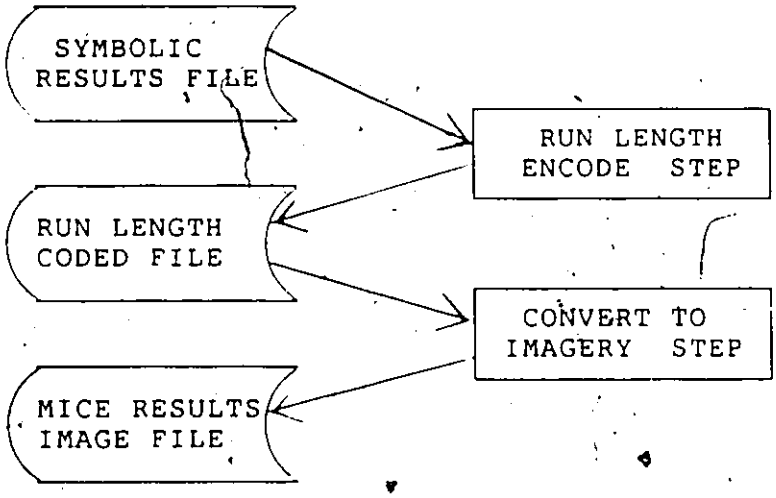

Figure 10 - The Post Processing Stage

7 DEMONSTRATION PROJECT

7.1 INPUT DATA

The Prince George area of British Columbia was selected as a study area for the map/image congruency evaluation experiment, as a number of data sets from a variety of sources were available for this area. The digital cartographic data from the British Columbia Ministry of Forests was obtained. This data contained the hydrography, cadastral, forest, roads, railroads and other cartographic information required for a forest cover map. The map scale was 1:20,000 and corresponded to the UTM map number 93G096. The BCMF forest cover map was received and stored as an Intergraph design file. This file contained a variety of cartographic information, but for the purposes of this experiment, only some of the map features were processed.

The Landsat MSS image (frame id: 50458-18360, orbit number: 6671) used in this experiment was imaged on June 25, 1985. The MSS image was then precision geocoded on the CCRS DICS system. The identification number of the map used in the geocoding was 093G15002. The radiometric parameters used in the generation of the product was a correction mode of sinx/x and a calibration type of LIN3 [MURPHY83]. The geocoded image was produced on the CCT PA3572. Figure 11 shows the location of the geocoded product relative to the original input CCT. Figure 12

shows the location of the map and the control points. Note that most of the map fits within the 20 metre RMS error contour interval. This means that the geocoded product should have 20 metre RMS spatial error. Since this translates to less than half a pixel (50x50 metres) RMS error, MICE assumes that the geocoded product is correct and thus no factor has been built in for geocoding error.

Figure 13 depicts the double line rivers and lakes level of the BCMF forest cover map. Figure 14 shows channel 4 of the Landsat MSS image that corresponds to the BCMF forest cover map.

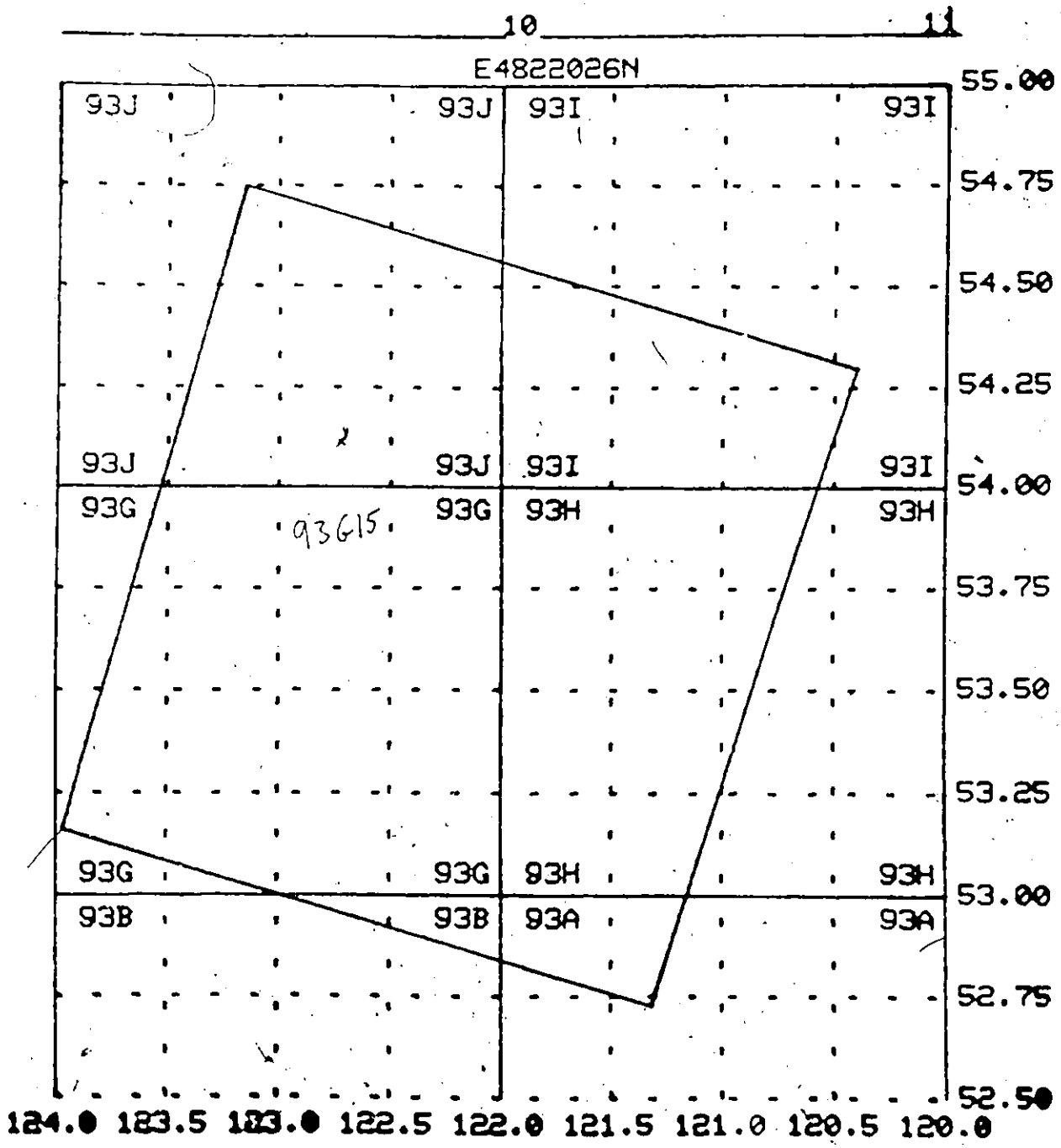

Figure 11 - Geocoded Image Positioning

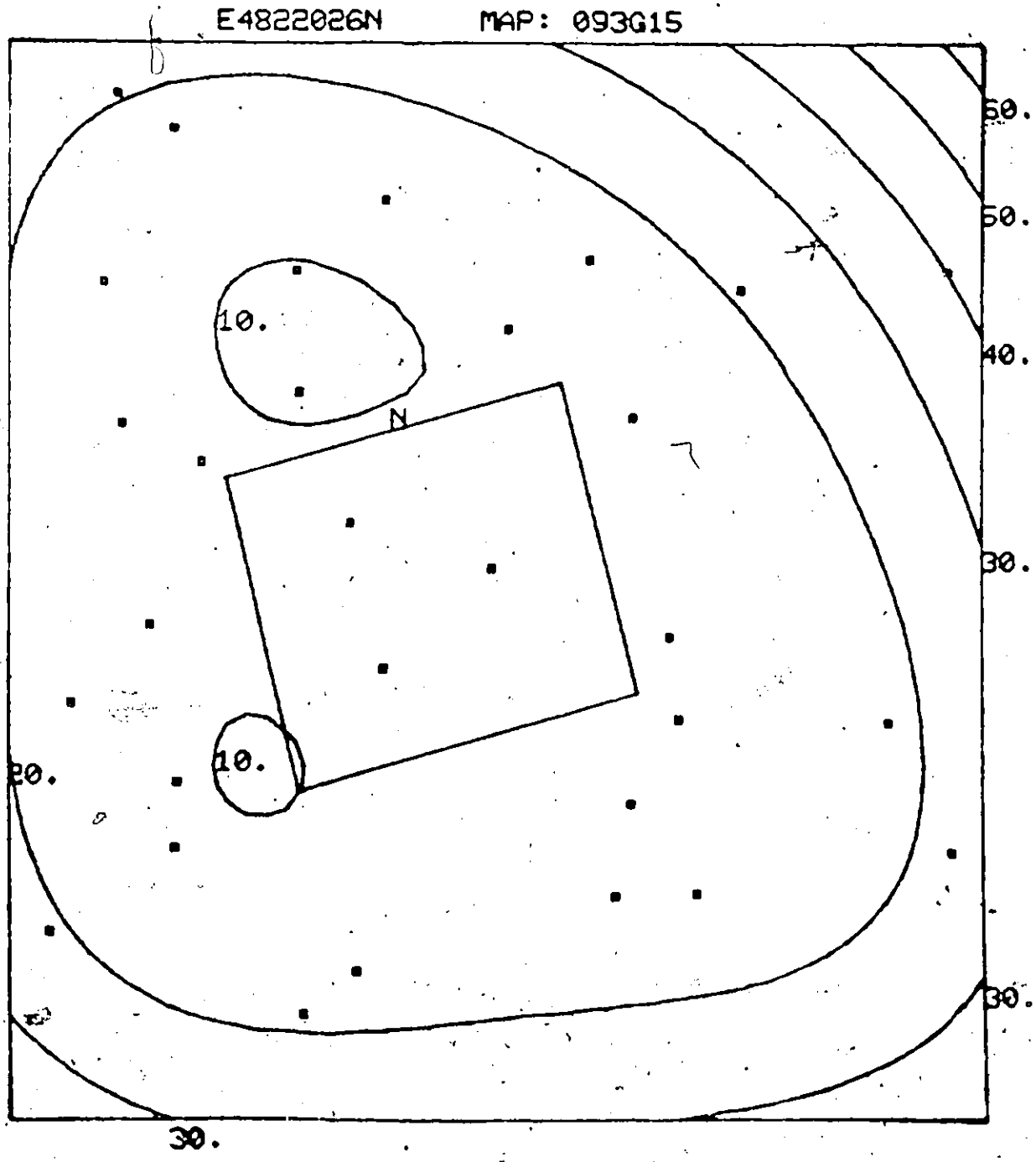

Figure 12 - Geocoded Image Control Points

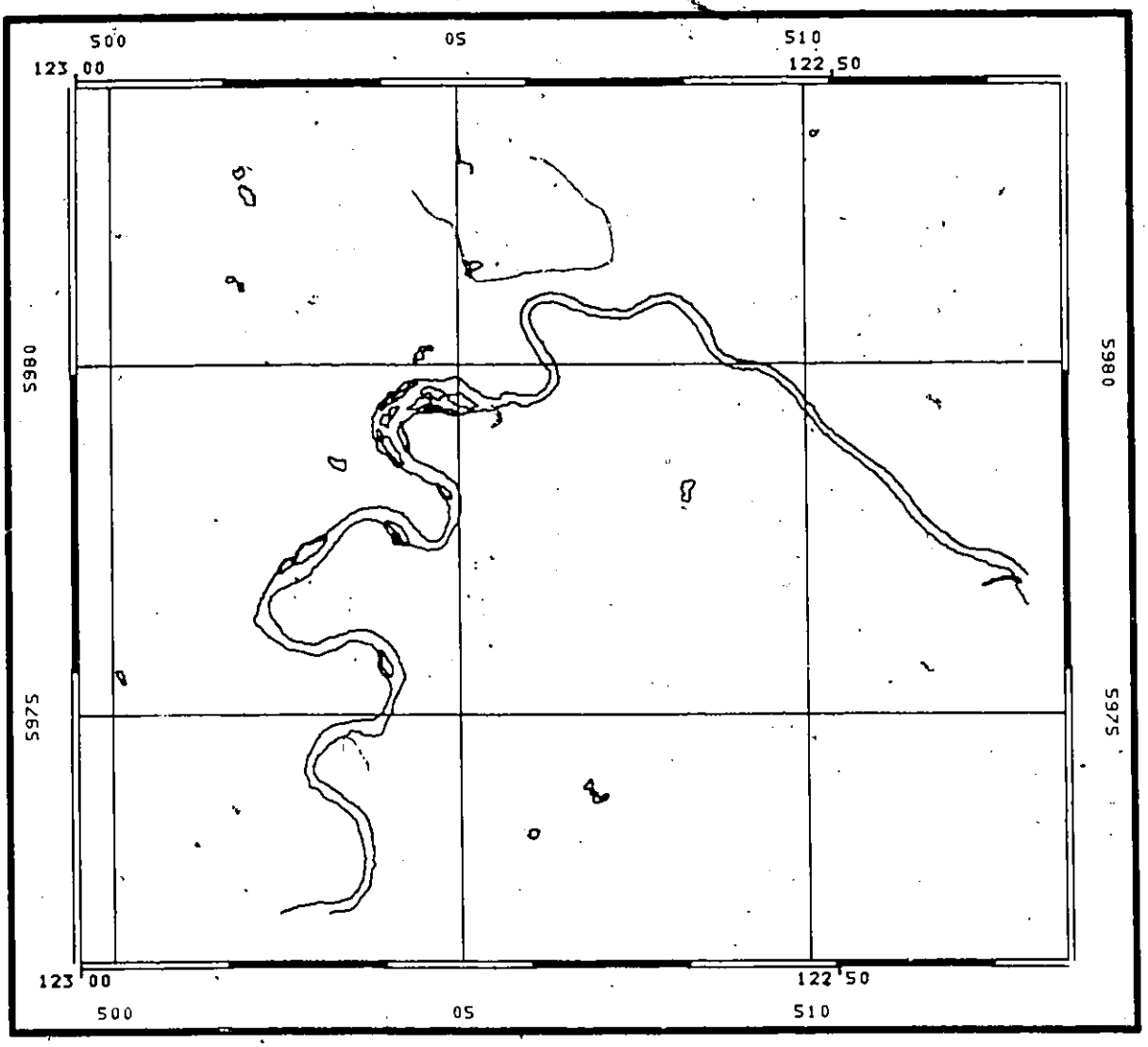

BCMF FOREST COVER MAP - HYDROLOGY LEVEL

SCALE 1:100000

MILES 2 4 6

KILOMETERS 5 10

Figure 13 - BCMF Map Double Line Rivers And Lakes

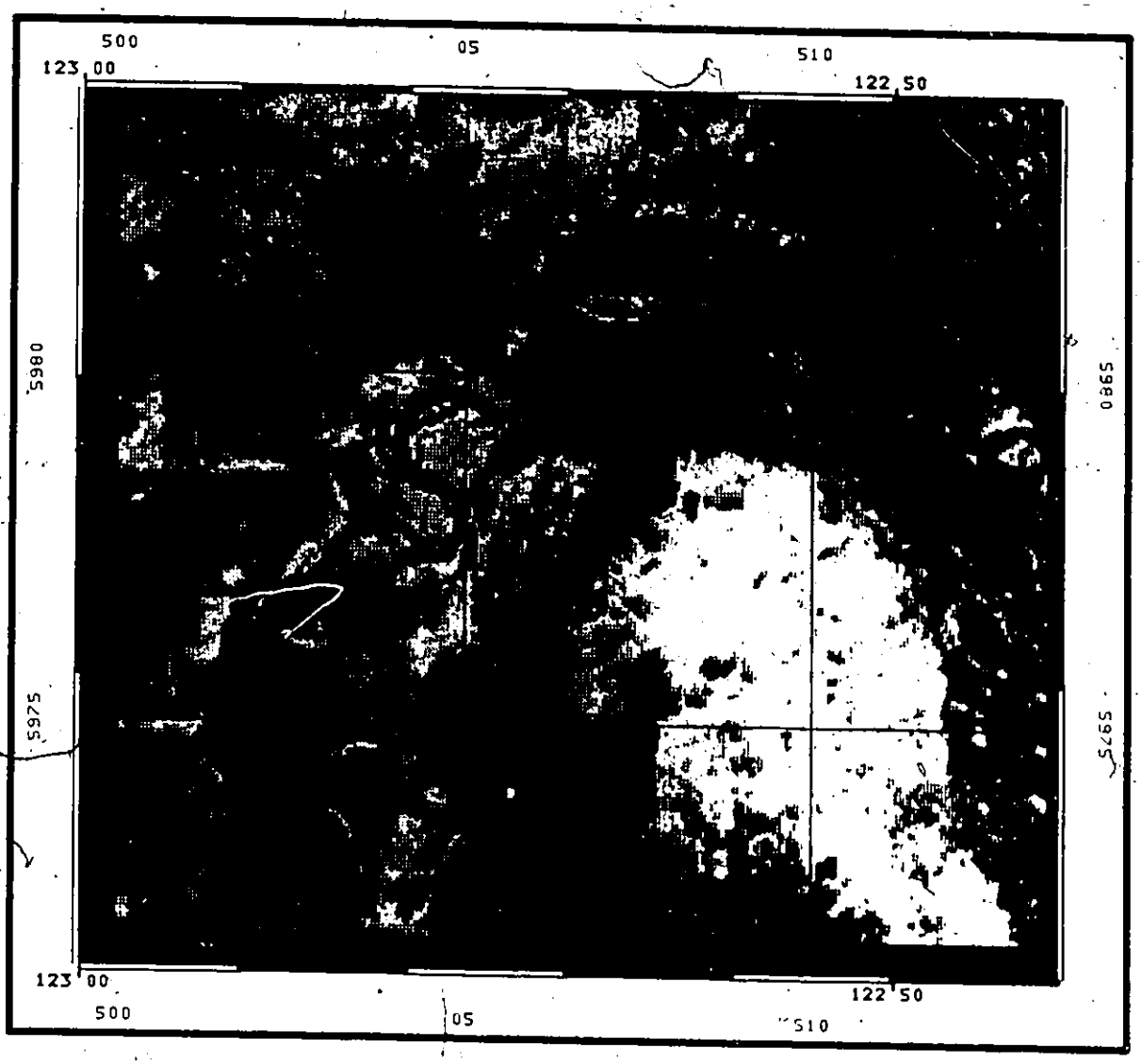

MSS CHANNEL 4 IMAGE

SCALE 1:100000

MILES 2 4 6

KILOMETERS 5 10

Figure 14 - Channel 4 Of Landsat MSS Image

7.2 MAP AND IMAGE PROCESSING

The BCMF forest cover map was received from BCMF on magnetic tape. The file 93G096.FC1 was copied from the tape onto an Intergraph Vax disk. The file was displayed on the Intergraph 68000 color graphics workstation. Level 6 of the BCMF forest cover map, which corresponds to double line rivers and lakes, was reviewed and all annotation text on that level was deleted. Next a cursor was precision placed around the map at the map working units shown in Figure 15.

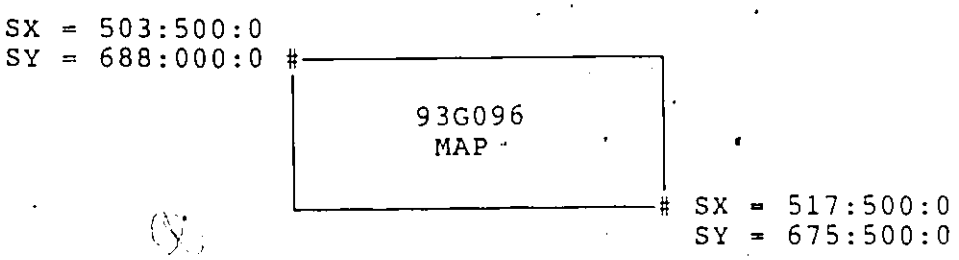

Figure 15 - BCMF Map Positional Information

Using the data inside this cursor, the file was run through a program to clean up any minor digitization errors. Next a polygon to grid program was executed using the presence/absence selection algorithm. Also, no rotation angle and a skew angle of 90 degrees along a 50 x 50 metre output grid was requested. The file 93G096.GRD was produced by the polygon to grid program. Next, a program was run to create the image format file 93G096.UNI. Then, the rasterized map was loaded onto a video display

and all the lakes and the Nechako river were digitally filled in, to create solid polygons. This filled polygon image was returned to the 93G096.UNI file.

The Landsat geocoded DICS image corresponding to the 93G096 forest cover map was received on a CCT. This tape was loaded onto a Vax disk and the sub-area roughly corresponding to the map was copied to the file 93G096.VID. Next, the MSS image and the BCMF map were precision registered. This was done by copying the map data to the 93G096.VID imagery file with no y-direction offset and with a 9 pixel x-direction offset. This offset was determined by evaluating the positional parameters of the upper left corner of the map and the image data. These positional parameters are depicted in Figure 16.

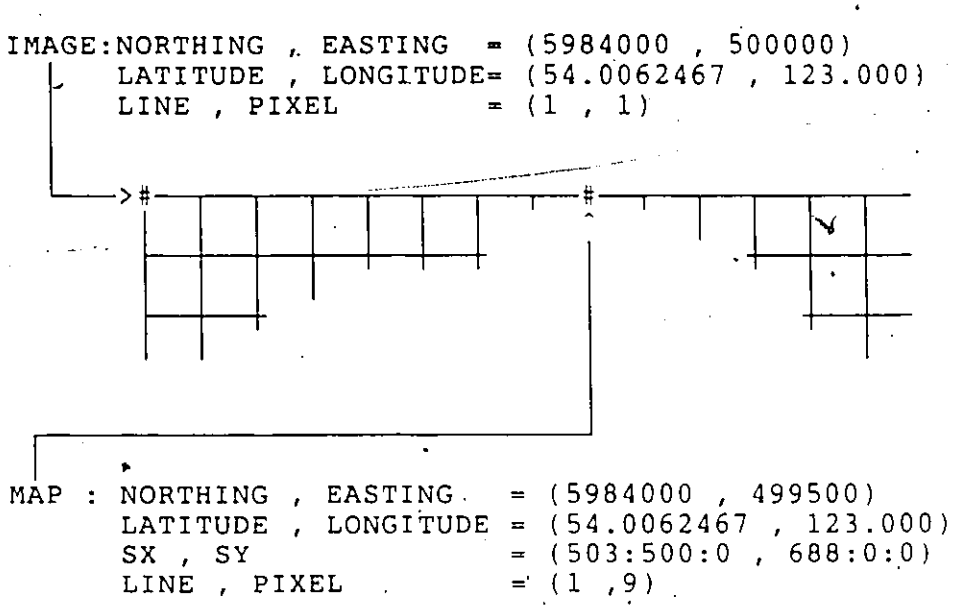

Figure 16 - Map / Image Precision Registration Parameters

Now that both the map and the image are registered to the same raster cartesian coordinate space, then the final processing can be done for creating the symbolic files. The map data was then run through a program, to convert the map segments to run-length encoded representation. Finally, the run-length encoded map segments were converted to a symbolic format file, along with the calculation of the segment size, shape and window attributes. This information was stored in the symbolic file MAPTRU.SYM.

Next, channel 4 of the MSS image was run through a 3 x 3 Sobel gradient operator and segmented, with a smoothing parameter set to segment only those segments that are surrounded by a fairly large gradient. This segmented

image was then passed through a program to generate a run-length encoded format file and then through a program to generate the image locations symbolic file IMGTRU.SYM. The image data was also passed through a program to generate the required Gaussian statistics of the segments. The image statistics symbolic file IMASTI.SYM was then generated.

The map symbolic file contained attributes on 13 map segments and the image symbolic files contained attributes on 319 image segments. These files were then input to the rule-based stage, which processed the attributes in the symbolic files and output the following symbolic results files: CLASS.RES, OVER.RES, SIZE.RES, SHAPE.RES. These files contain the image segments that were determined to be in the same class, overlapped the map segment, were of similar size to the map segment or were of similar shape to the map segment, respectively.

The symbolic results files were converted to run-length encoded format files and were then converted to image format. The resulting image files could be loaded onto the video display and viewed or further evaluated as required.

7.3 EXPERIMENT RESULTS AND EVALUATION

Figure 17a shows the BCMF forest cover map following editing and rasterization. Note that each map segment has been numbered with its corresponding segment number. When the rasterized map (Figure 17a) is visually compared to the original vector map (Figure 13), it can be seen that the lakes and rivers have been filled in. Figure 17b compares the BCMF raster map and the BCMF vector map. Figure 18 depicts the results of segmenting channel 4 of the Landsat image using the Sobel operator. Note that the segment shading is for display purposes only, so that no two neighboring segments have the same shade.

Figure 19 shows the image segments from Figure 18 that were selected as being approximately the same size as the corresponding map segment of Figure 17a. Note that only 5 segments were located as being approximately the same size.

Figure 20 shows the image segments from Figure 18, that were selected as being approximately the same shape as the corresponding map segment of Figure 17a. Note that 12 image segments were located as being approximately the same shape.

Figure 21 shows the image segments from Figure 18, that were selected as being classified as hydrography. Note that several lakes and most of the Nechako River were located.

Figure 22 shows the image segments from Figure 18, that overlapped with any map segment, irregardless of class, size or shape. Note that many segments were located including the large landmass segments.

Figures 23, 24, 25, and 26 show how the similar size, similar shape, same class and overlap segments, respectively, compared with the BCMF vector map of Figure 13.

The MICE user can decide on the congruency of the map and the image by evaluating various combinations of the results data shown in Figures 19 through 22, with the rasterized map of Figure 17a. Table 5 shows the matching segments for the sample run given in section 10. Table 6 compares the locations and overlap for the segments from Table 5, for which there were at least three matching attributes. Note that there are no consistent x-direction or y-direction displacements. Thus we can conclude that for this sample run, the map and the image are congruent, as expected.

MAP SEGMENT	SAME CLASS IMAGE SEGMENTS	SIMILAR SIZE IMAGE SEGMENTS	SIMILAR SHAPE IMAGE SEGMENTS	OVERLAP IMAGE SEGMENTS
[2]	[]	[]	[]	[2]
[9]	[]	[]	[]	[2]
[7]	[]	[]	[]	[2]
[11]	[]	[]	[]	[2]
[12]	[]	[296]	[296]	[296,54]
[1]	[]	[25]	[25]	[25,2]
[10]	[138]	[138]	[145,142, 138,137, 129]	[138,2]
[4]	[40]	[]	[41]	[41,40,2]
[5]	[]	[74]	[74,70]	[74,72,70, 2]
[3]	[146]	[146]	[146]	[146,54]
[6]	[31]	[]	[31,25]	[31,2]
[13]	[]	[]	[]	[54]
[14]	[316,313, 310,309, 302,298, 293,290, 282,279, 276,275, 270,269, 266,264, 262,245, 238,233, 229,228, 227,226, 223,222, 219,218, 211,206, 204,199, 198,197, 194,193, 192,191, 190,188, 185,183,	[]	[]	[316,314, 313,310, 309,306, 304,302, 298,294, 293,292, 291,290, 288,282, 279,276, 275,272, 270,269, 266,264, 262,256, 248,245, 238,233, 229,228, 227,226, 223,222, 219,218, 211,209, 206,204,

```
179,177,
175,174,
173,171,
167,166,
160,159,
158,157,
156,155,
153,152,
147,146,
144,143,
141,140,
139,138,
136,135,
133,128,
122,118,
114,111,
103,102,
101,99,
98,93,
91,90,
88,87,
85,84,
81,80,
79,78,
77,76,
73,71,
69,67,
65,63,
62,61,
60,58,
57,56,
55,51,
50,48,
47,46,
45,44,
40]
```

```
198,197,
196,195,
194,193,
192,191,
190,189,
188,185,
184,183,
179,177,
176,175,
174,173,
171,169,
167,166,
163,162,
160,159,
158,157,
156,155,
154,153,
152,147,
144,143,
141,140,
139,136,
135,134,
133,132,
131,128,
126,125,
122,119,
118,117,
114,113,
112,111,
110,109,
108,107,
105,104,
103,102,
101,100,
99,98,
97,95,
93,92,
91,90,
88,87,
85,84,
82,81,
80,79,
78,77,
76,73,
71,69,
67,65,
63,62,
61,60,
58,57,
56,55,
54,51,
50,49,
48,47,
46,45,
44,42,
```

| | | | 21

Table 5 - Table of Matching Segments

MAP SEGMENT	12	1	10	5	3	6
MATCHING IMAGE SEGMENT	296	25	138	74	146	31
NUMBER OF OVERLAP PIXELS	7	5	14	8	12	10
NUMBER OF PIXELS IN MAP AND NOT IN IMAGE	5	8	6	14	13	19
NUMBER OF PIXELS IN IMAGE AND NOT IN MAP	2	8	4	8	6	6
IMAGE SEGMENT CENTRE	[214, 130]	[45, 26]	[76, 109]	[101, 78]	[174, 117]	[48, 32]
MAP SEGMENT CENTRE	[214, 131]	[48, 26]	[76, 109]	[100, 77]	[176, 117]	[50, 32]
CENTRE X-OFFSET	0	-3	0	1	-2	-2
CENTRE Y-OFFSET	-1	0	0	1	0	0

Table 6 - Table of Congruency Evaluation

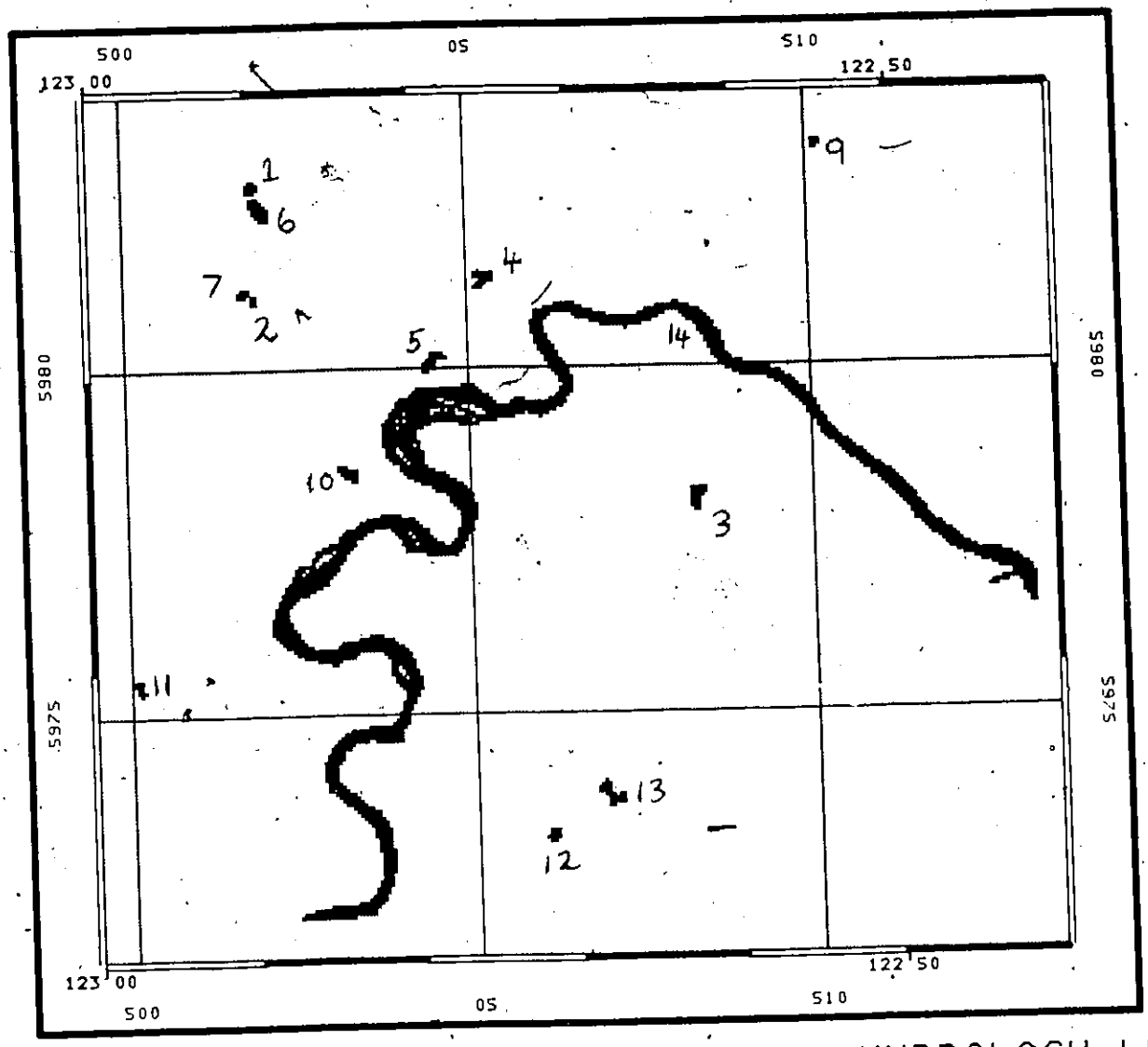

RASTERIZED BCMF FOREST COVER MAP - HYDROLOGY LEVEL

SCALE 1:100000

MILES 2 4 6

KILOMETERS 5 10

Figure 17a - BCMF Map After Editing and Rasterization

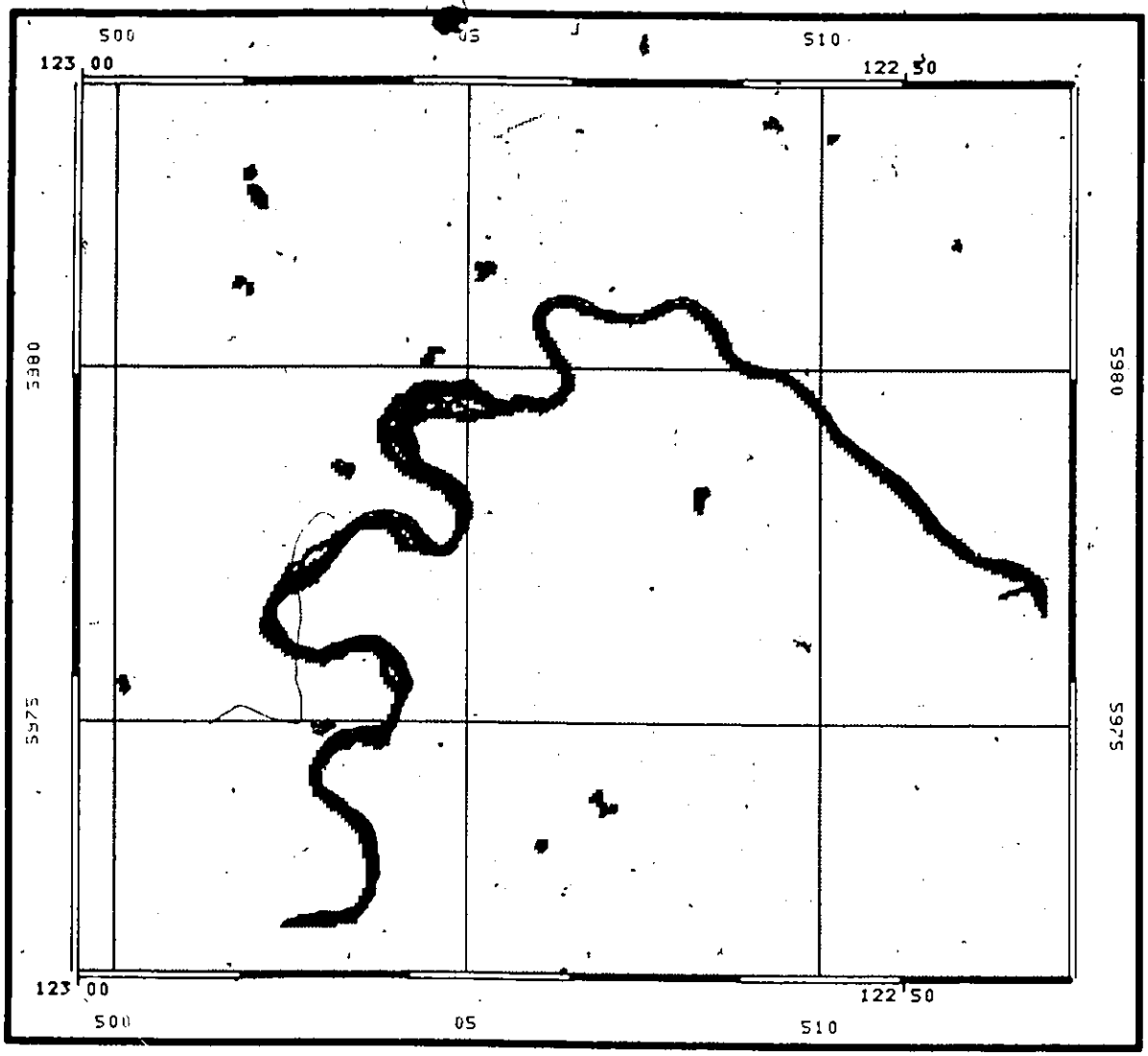

RASTERIZED BCMF MAP COMPARED TO VECTOR MAP

SCALE 1:100000

MILES 2 4 6

KILOMETERS 5 10

Figure 17b - BCMF Raster Map Compared With Vector Map

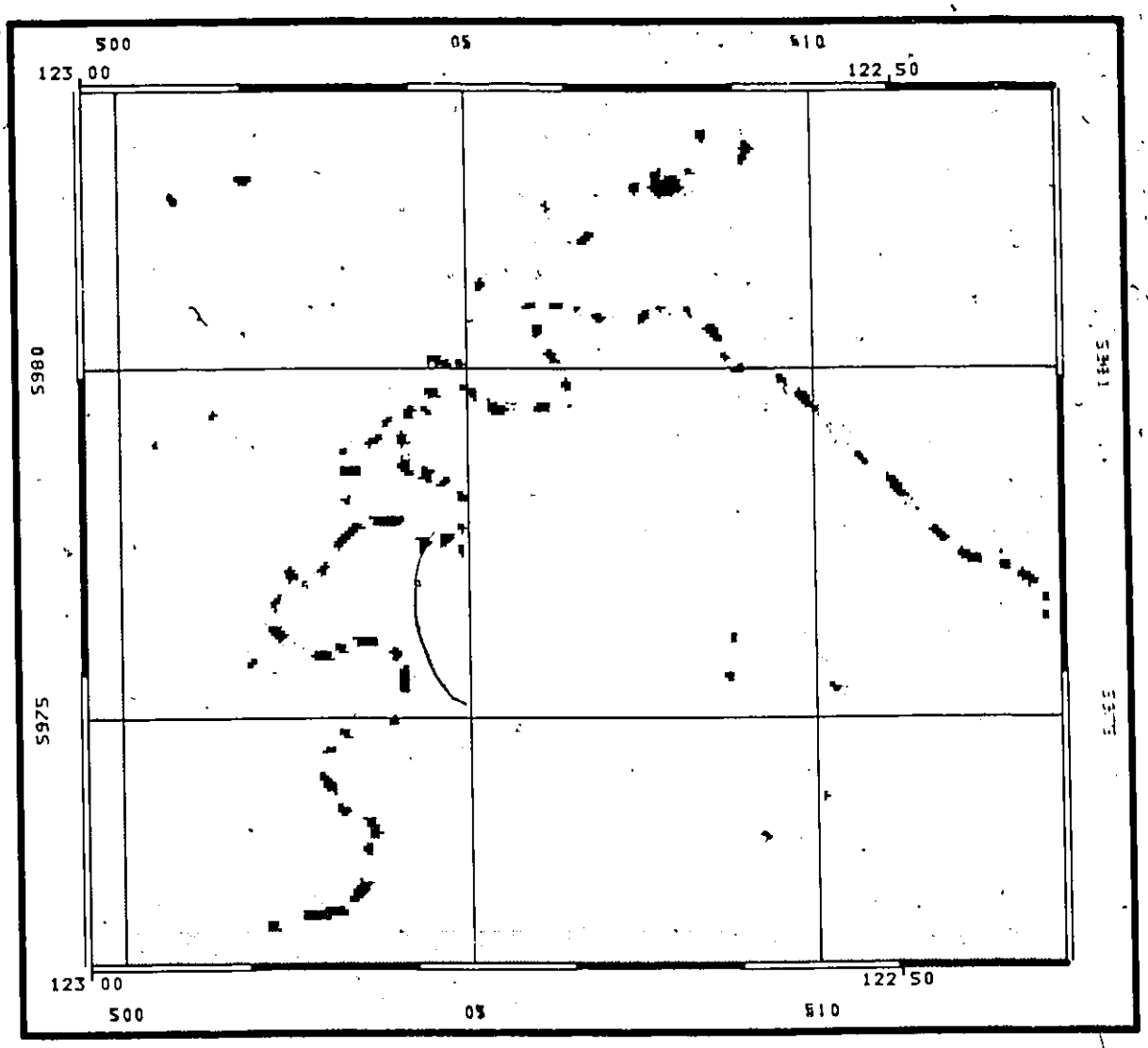

SEGMENTED MSS CHANNEL 4 IMAGE

SCALE 1:100000

MILES 2 4 6

KILOMETERS 5 10

figure 18 - MSS Channel 4 Following Segmentation

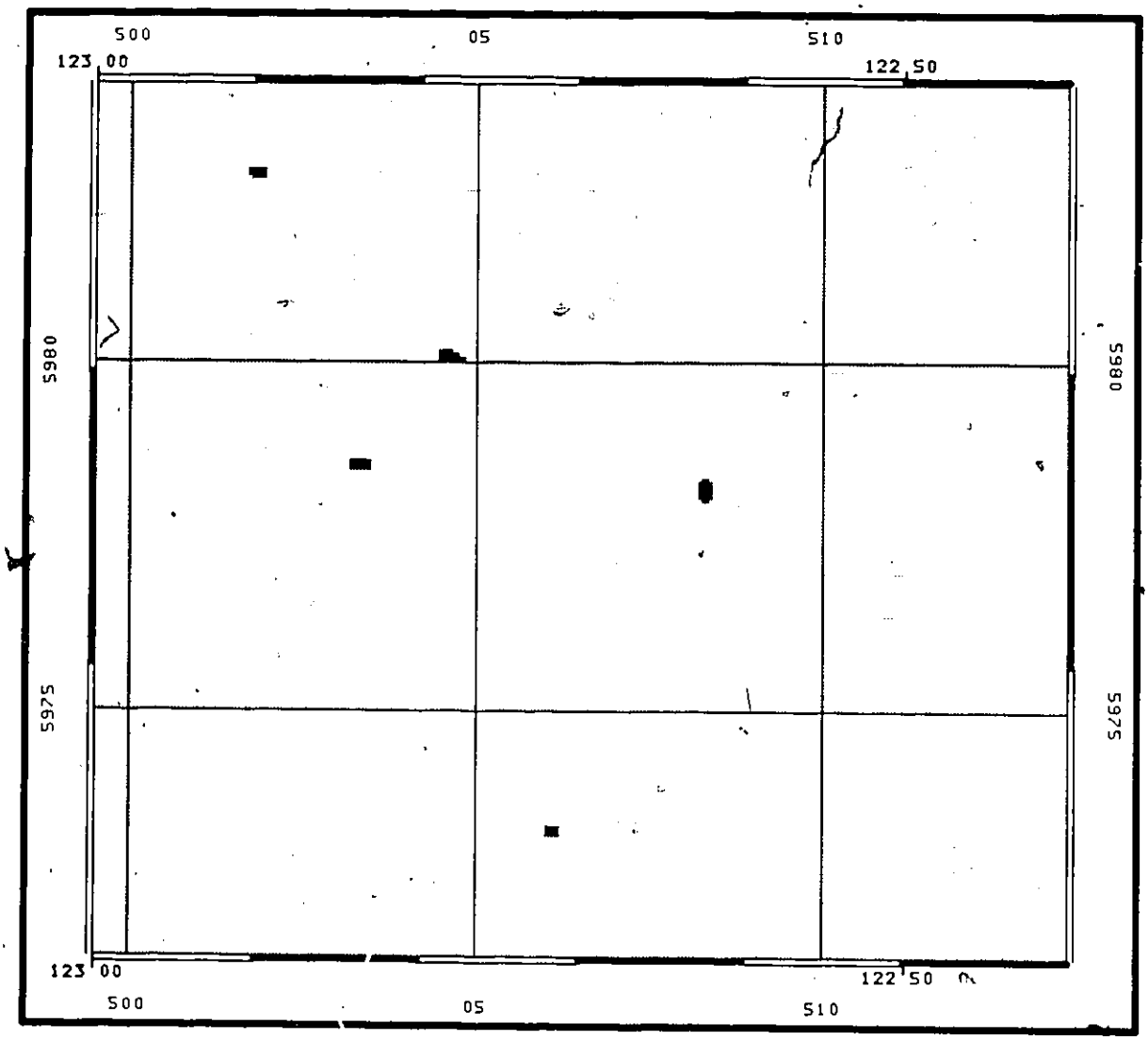

figure 19 - MSS Segments Selected As Being Approximately The Same Size

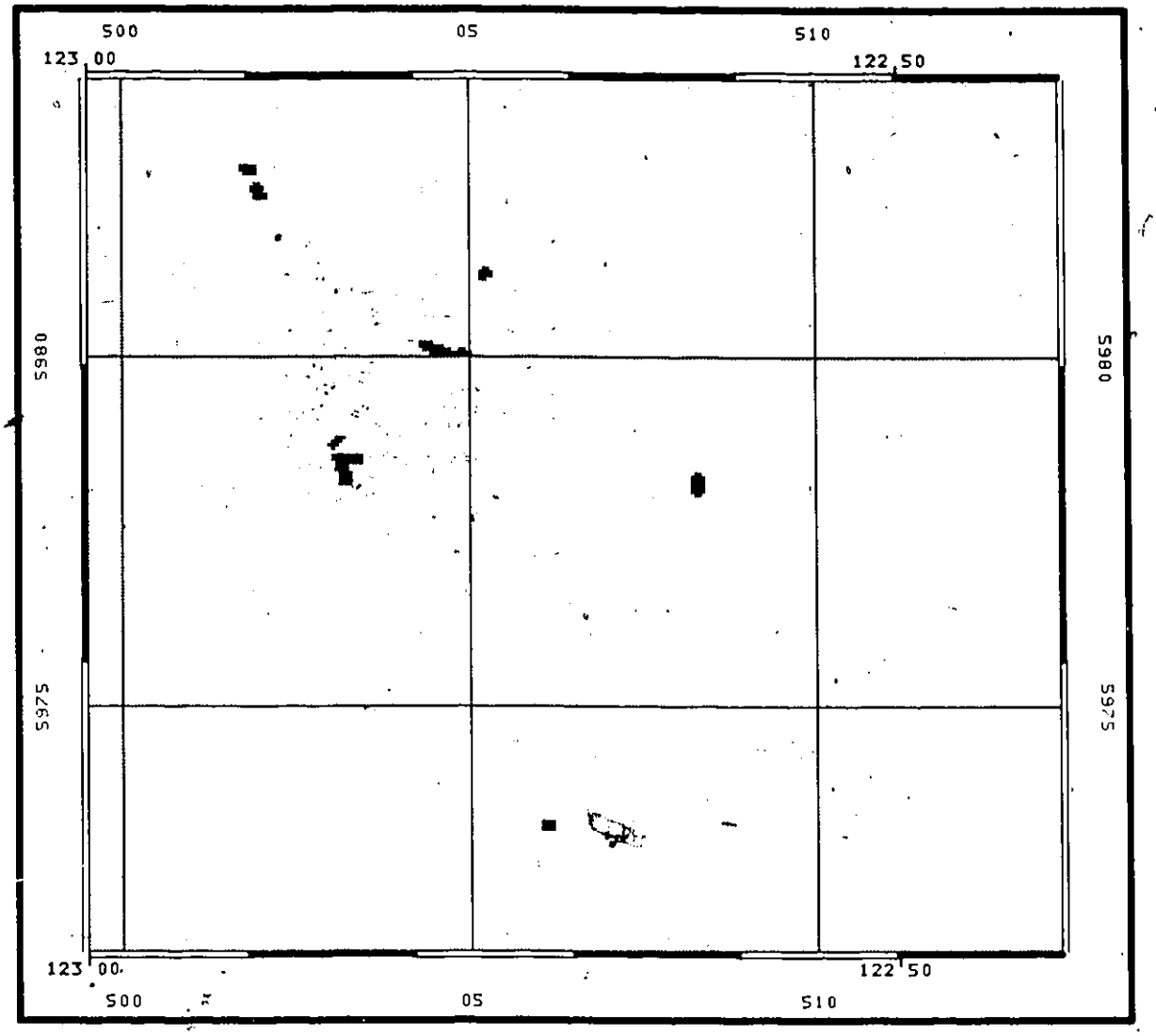

MSS SEGMENTS SELECTED AS SIMILAR SHAPE

SCALE 1:100000

MILES 2 4 6

KILOMETERS 5 10

figure 20 - MSS Segments Selected As Being Approximately The Same Shape

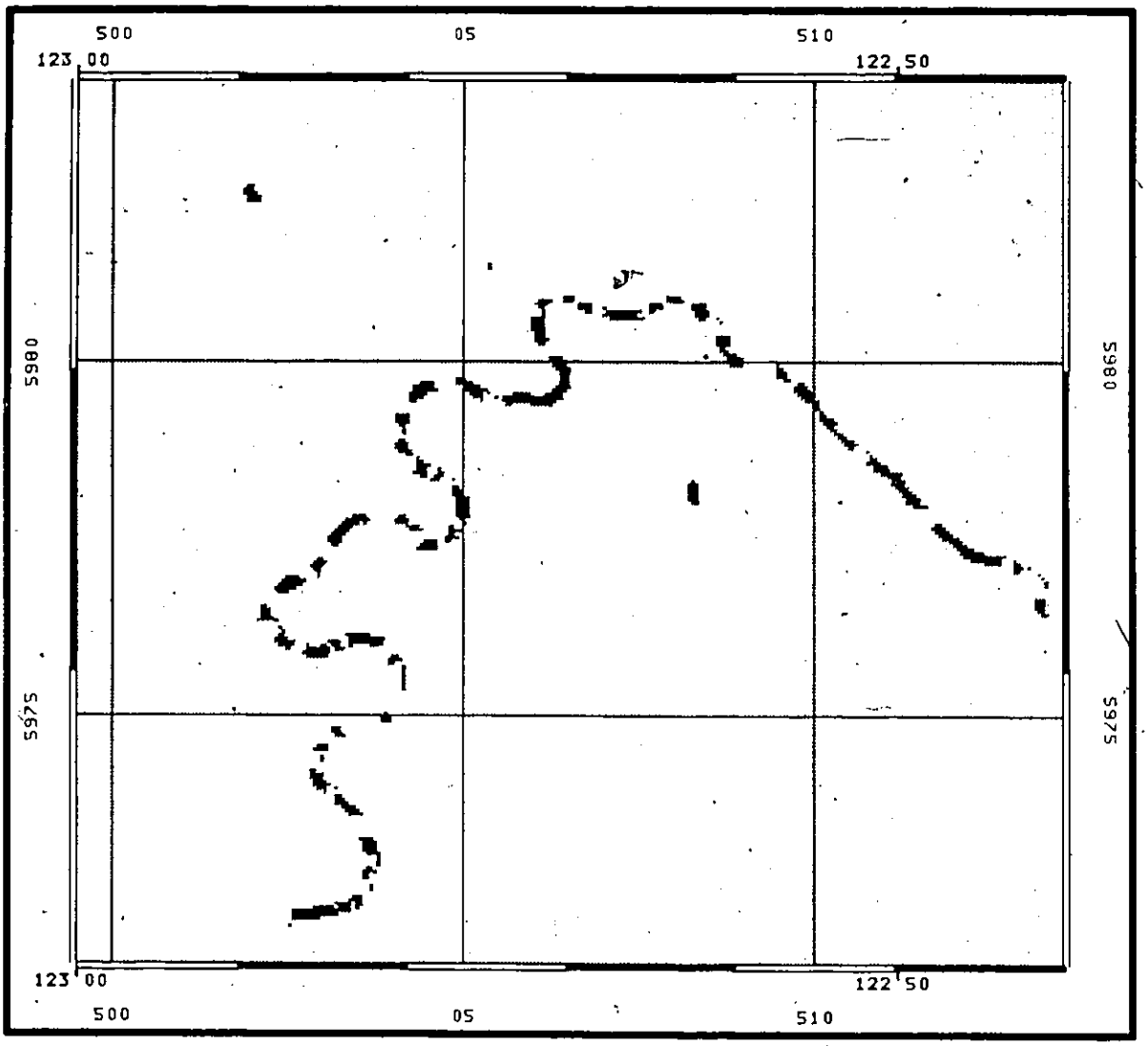

MSS SEGMENTS CLASSIFIED AS HYDROGRAPHY

SCALE 1:100000

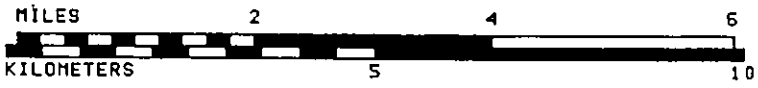

figure 21 - MSS Segments Selected As Classified As Hydrography

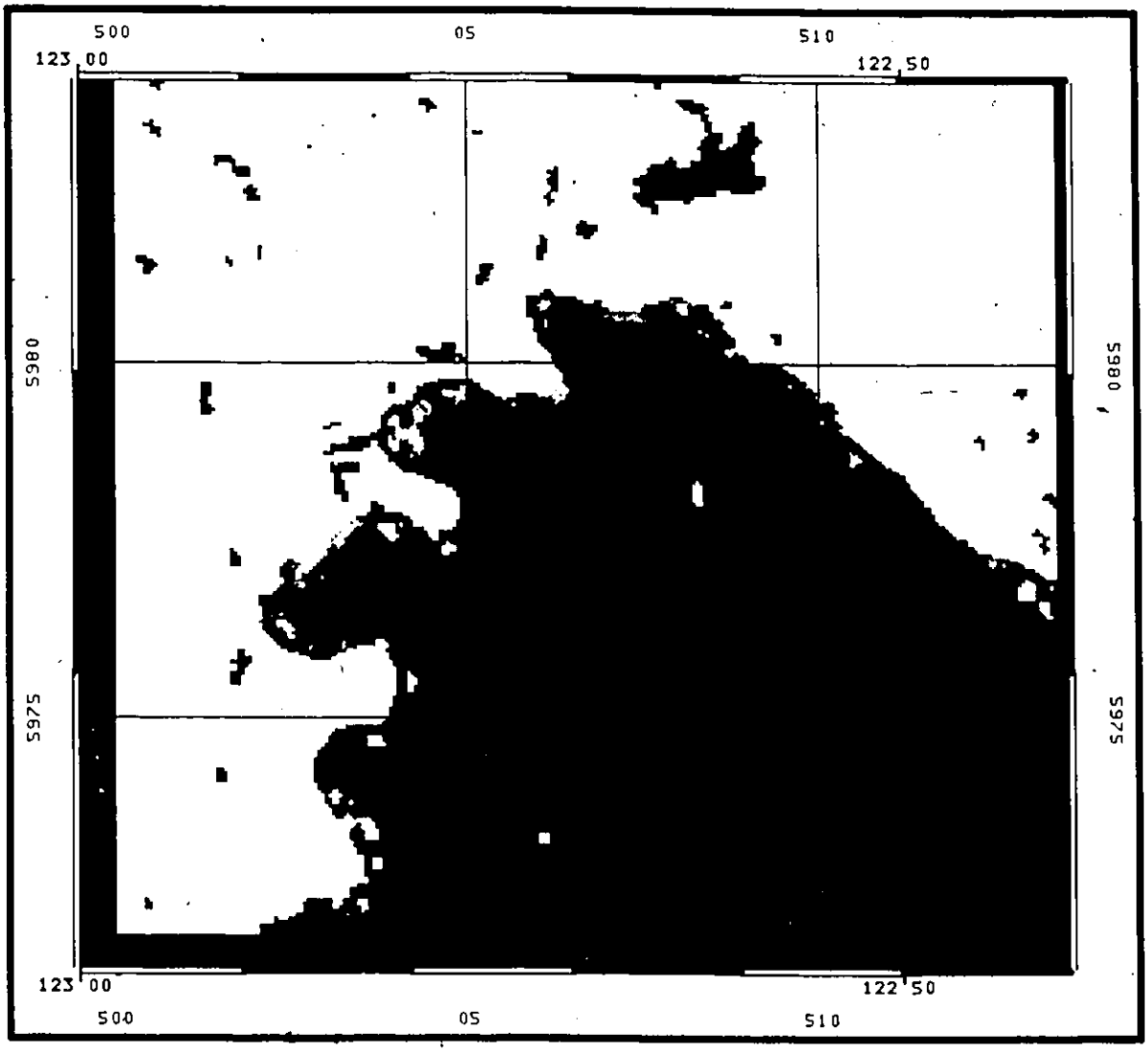

MSS SEGMENTS SELECTED AS OVERLAPPING MAP SEGMENTS

SCALE 1:100000

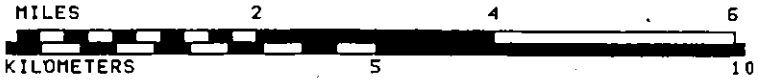

figure 22 - MSS Segments Selected As Overlapping Map Segment

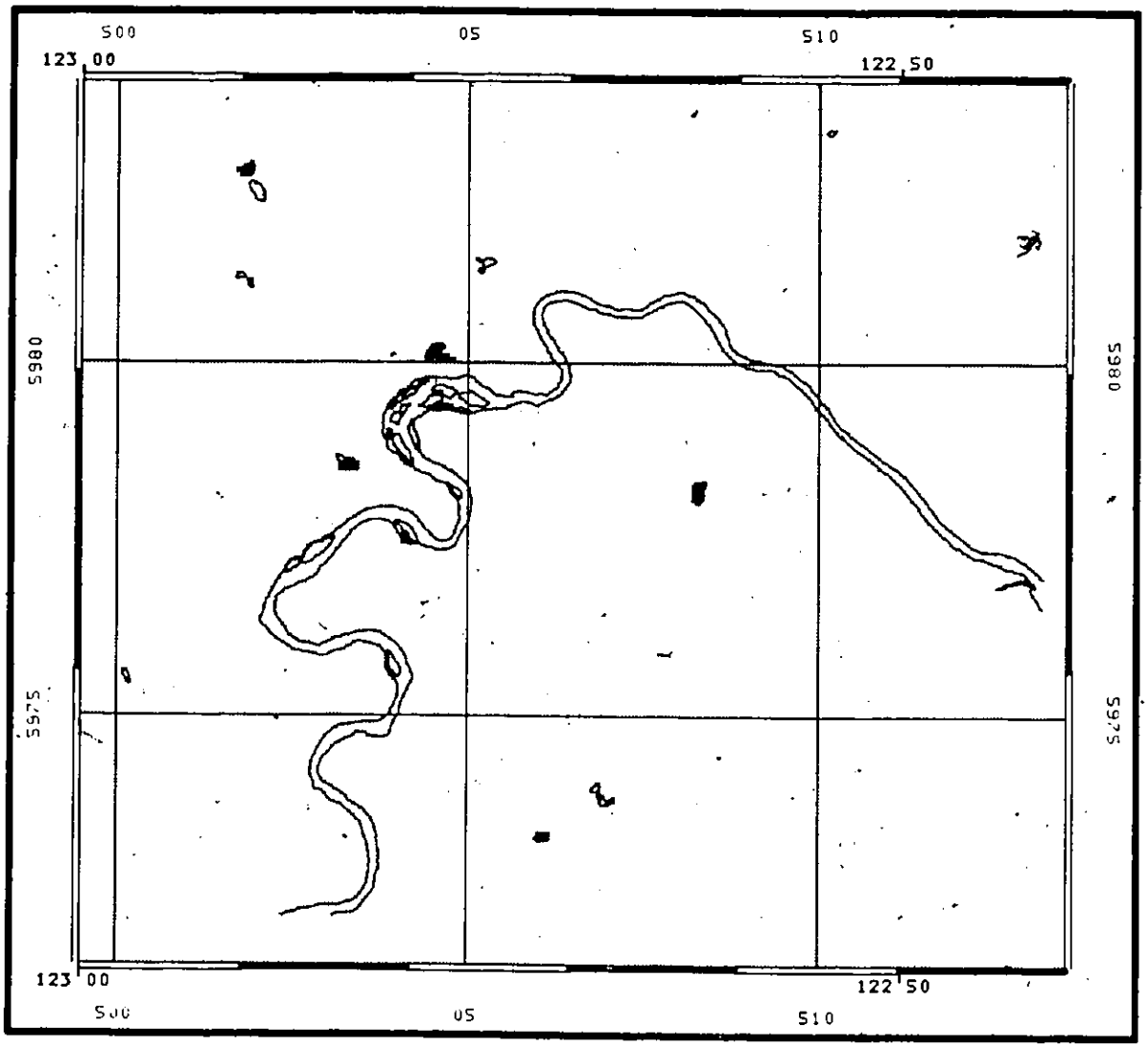

SIMILAR SIZE SEGMENTS COMPARED TO BCMF MAP

SCALE 1:100000

MILES 2 4 6

KILOMETERS 5 10

figure 23 - Size Selected Segments Compared With BCMF Map

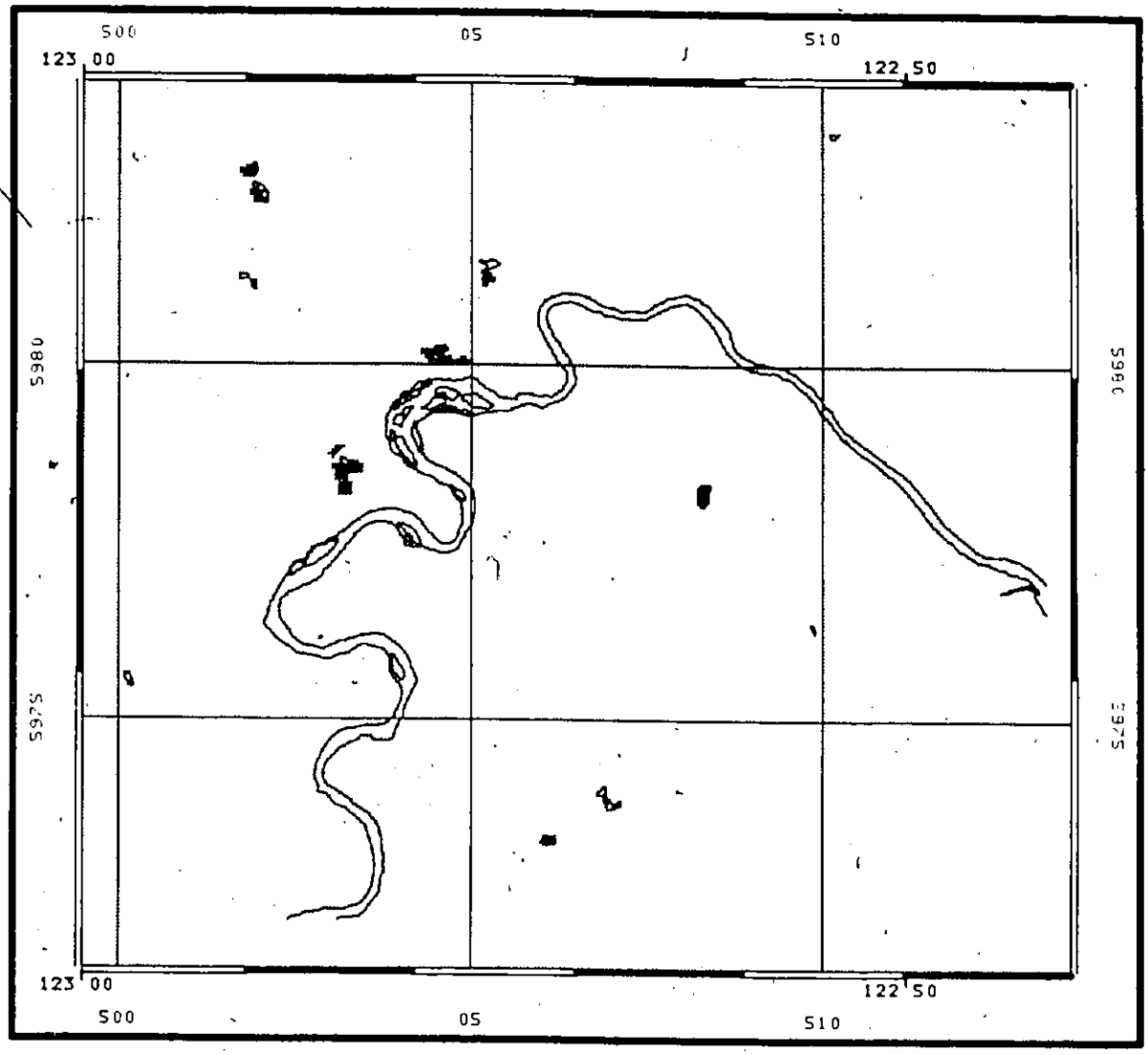

SIMILAR SHAPE SEGMENTS COMPARED TO BCMF MAP

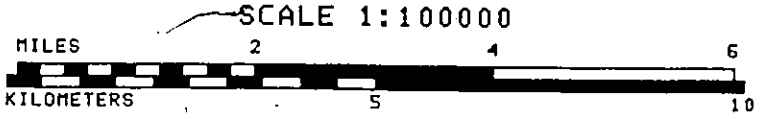

figure 24 - Shape Selected Segments Compared With BCMF Map

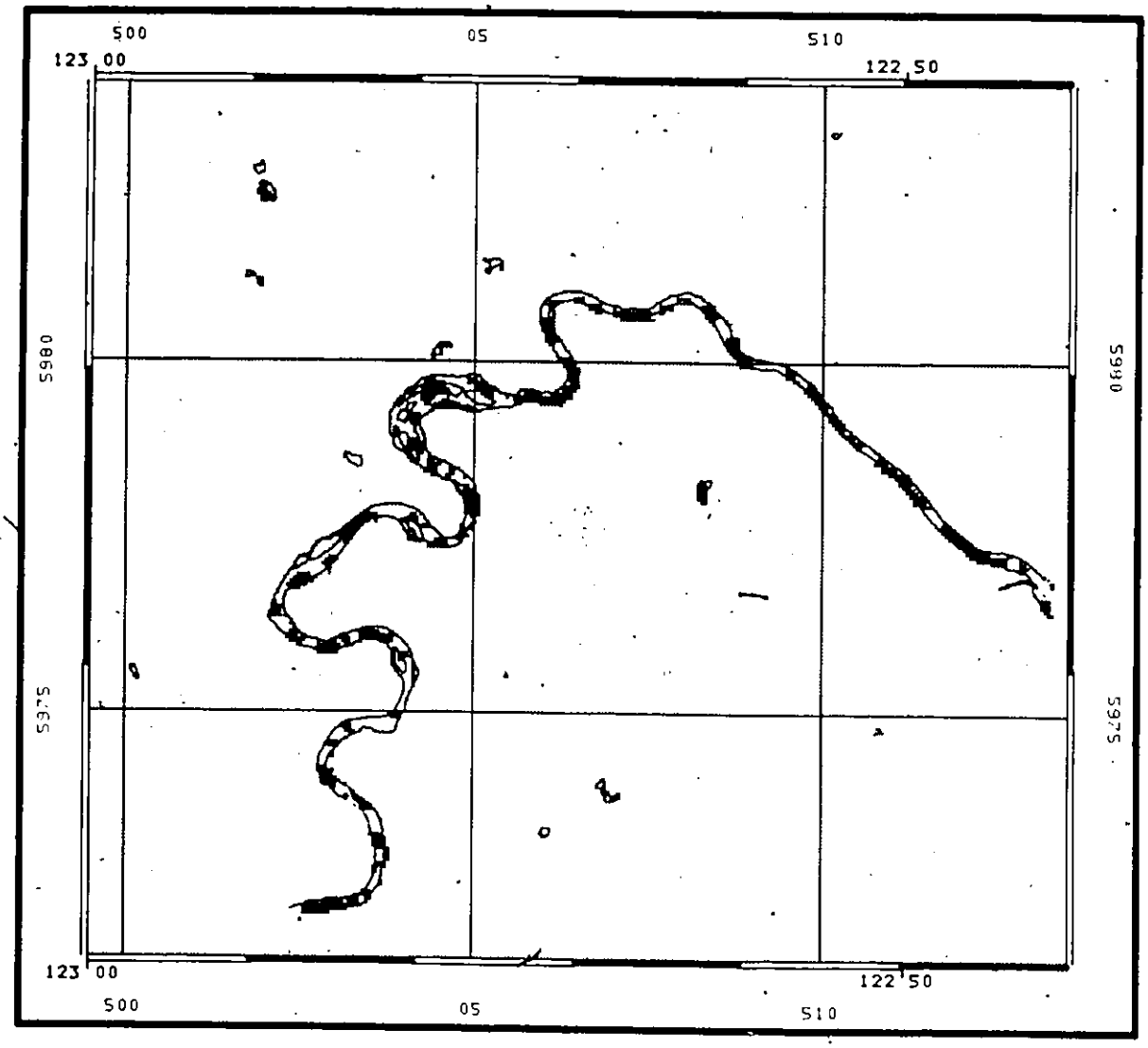

CLASSIFIED SEGMENTS COMPARED TO BCMF MAP

SCALE 1:100000

MILES 2 4 6

KILOMETERS 5 10

figure 25 - Hydrography Classified Segments Compared With BCMF Map

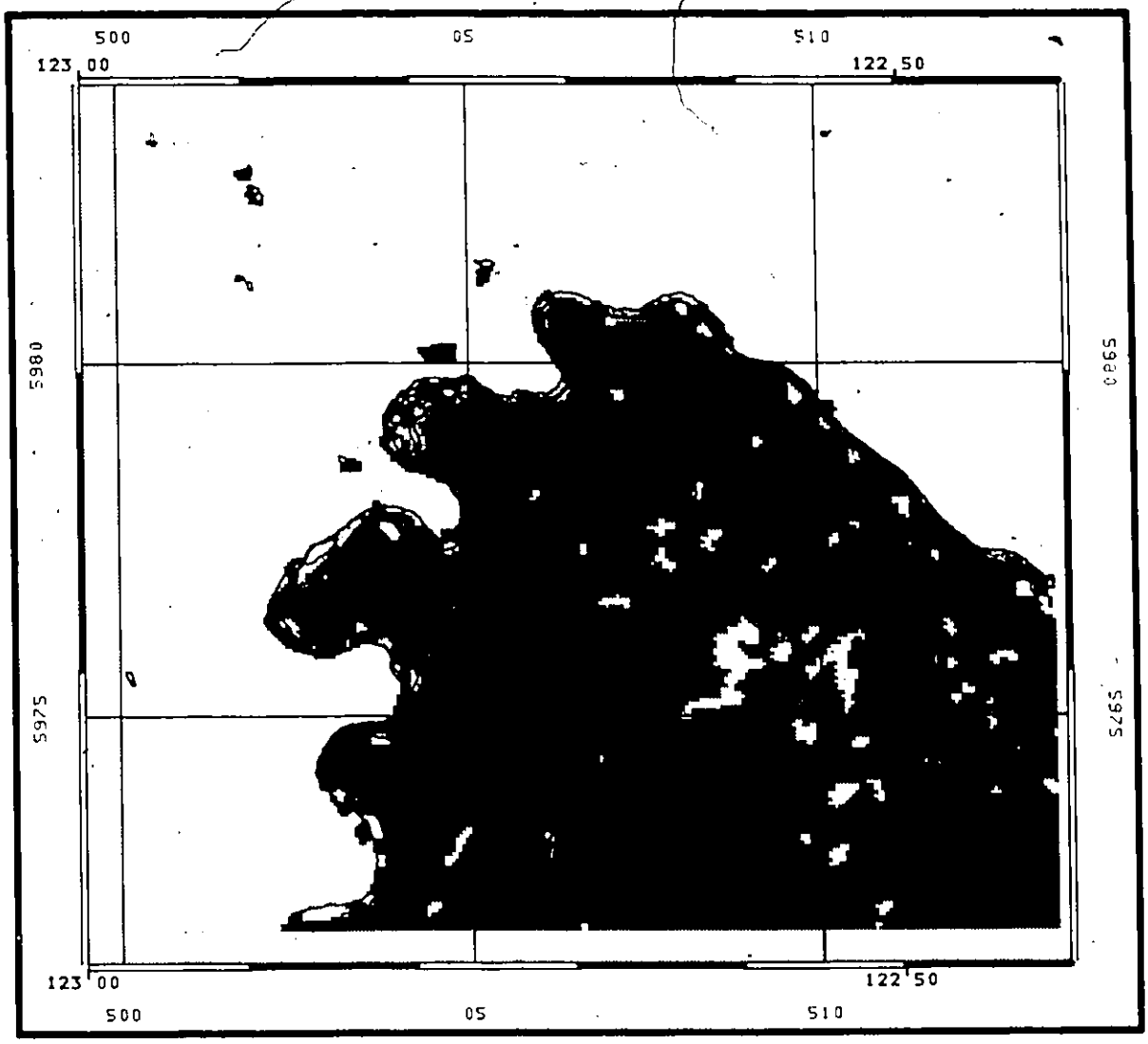

OVERLAPPING SEGMENTS COMPARED TO BCMF MAP

SCALE 1:100000

MILES 2 4 6

KILOMETERS 5 10

figure 26 - Overlapping Image Segments Compared With BCMF Map

8 SUMMARY AND CONCLUSIONS

The following conclusions can be drawn from the work performed thus far:

1. The results so far are very favourable for performing map/image comparisons using an artificial intelligence / knowledge based system approach. The only drawback appears to be the throughput rate. Currently the PROLOG stage of the analysis takes approximately three hours on a VAX AI workstation, to analyse one level. There have not yet been any performance enhancements to the PROLOG code, so this timing figure could improve significantly.

2. There is a great deal of fiddling and reformatting steps in the preprocessing and postprocessing stages. Many steps in these stages could be eliminated if some new software was developed to perform many steps at once.

3. The size heuristic does not appear to add much to the congruency evaluation. However when additional rules for splitting and merging of image and map segments are available, then this should be a more worthwhile heuristic. Splitting and merging segments will allow the segments to increase in size or decrease in size as dictated by the split or merge heuristic. For example in

the experiment results discussed here, if the segments in the river were merged, because these adjacent segments were the same class, then the merged segment would have matched in size with the map river segment.

4. The shape heuristic as is, does provide some clues to the identification of the corresponding image segment. However better shape descriptor attributes, such as Fourier descriptors or others could improve the image segment selection.

5. The classification heuristic appears to give good results for the water class. However further study and better rules for other classes would improve the image segment selection.

6. The overlap heuristic appears to give good results when the map and the image are very close to matching. It is unclear if this heuristic would be of much value, if there was a great deal of misregistration.

7. Better results for the congruency evaluation are anticipated when a geocoded Landsat thematic Mapper image is used in the experiment. The improved spectral resolution should help in class discrimination and the improved spatial resolution should provide more accurate congruency evaluation results.

8. Additional experiments using EMR topographic map data for this area would provide additional insight into the map/image congruency evaluation problem.

9 REFERENCES

1. [BASDEN84] Basden, A.; "On The Application of Expert Systems"; Developments in Expert Systems, Coombs, M.J. (ed); 1984; pp 59-75.

2. [BILLINGSLEY82] Billingsley, F.C.; "Edited Oral Presentation"; Proceedings of the NASA Workshop on Registration and Rectification; Bryant, N.A.(ed); NASA-JPL Publication 82-23; June 1982; pp 13-20.

3. [BEAULIEU85] Beaulieu, J.M. and Goldberg, M.; "A Selection of Segmentation Similarity Measures for Hierarchical Picture Segmentation"; Graphics Interface; May 1985; pp 179-186.

4. [BOYLE80] Boyle, A.R.; "Scan Digitization of Cartographic Data"; Map Data Processing, Freeman, H. (ed) and Pieroni, G.G. (ed); 1980; pp 27-46.

5. [BRAUN85] Braun, F.; University of Ottawa, MASC Thesis; 1985.

6. [BRYANT82] Bryant, N.A. (ed); "Proceedings of the NASA Workshop on Registration and Rectification"; NASA-JPL publication 82-23; June 1982; pp 517.

7. [COOMBS84] Coombs, M.J. (ed); "Developments in Expert Systems"; Academic Press; 1984; Preface.

8. [DUDA79] Duda, R.O., Hart, P.E., Konolige, K. and Reboh, R.; "A Computer-based Consultant for Mineral Exploration"; Technical Report, SRI International, September 1979.

9. [ERMAN80] Erman, L.D., Hayes-Roth, F., Lesser, V.R. and Reddy, D.R.; "The Hearsay-II Speech understanding System: Integrating Knowledge to Resolve Uncertainty"; Computing Surveys, Vol 12, No. 2; June 1980, pp 213-253.

10. [GEVARTNER82] Gevartner, W.B.; "An Overview of Expert Systems"; NBSIR 82-2505; National Bureau of Standards, Department of Commerce; May 1982.

11. [GLICKSMAN82] Glicksman, J.; "A Cooperative Scheme For Image Understanding Using Multiple Sources Of Information" PhD Thesis, University Of British Columbia; November 1982.

12. [GOLDBERG85] Goldberg, M., Goodenough, D.G., Alvo, M. and Karam, G.; "A Heirarchical Expert System For Updating Forestry Maps With Landsat Data"; Proceedings of the IEEE, Vol 73, No 6; June 1985; pp 1054-1063.

13. [GOODALL85] Goodall, A.; "The Guide To Expert Systems"; Learned Information, May 1985.

14. [GOODENOUGH85] Goodenough, D.G., Fung, K.B., Hegyi, F., Robson, M. and Swanberg, N.A.; "Integration Of Geographic Information Systems with Landsat Thematic Mapper Data"; paper presented at IGARSS'85.

15. [GUERTIN81] Guertin, F.E. and Shaw, E.; "Definition and Potential of Geocoded Satellite Imagery Products"; presented at the 7th Canadian Symposium on Remote Sensing; September 1985; pp 384-394.

16. [HANSON78] Hanson, A.R. and Riseman, E.M.; "VISIONS: A Computer System For Interpreting Scenes"; Computer Vision Systems, Hanson, A.R. (ed) and Riseman, E.M. (ed); Academic Press; 1978; pp 303-334.

17. [HEGYI83] Hegyi, F. and Sallaway, P.; "Integration Of Vector And Grid Data Bases In B.C. Forest Inventory"; Proceedings of the Sixth International Symposium on Automated Cartography; Wellar, B.S.(ed); October 1983; pp 215-221.

18. [LETENDRE85] Letendre, A.; "Expert Systems"; Report No. 1/85; Office of Industrial Innovation, Department of Regional Industrial Expansion, Government of Canada; October 1985.

19. [LEVINE86] Levine, M.D. and Hong, W.; "A Knowledge-Based Approach to Computer Vision Systems"; Graphics/Vision Interface; May 1986; pp 260-265.

20. [LINDSAY80] Lindsay, R., Buchanan, B.C., Feigenbaum, E.A. and Lederberg, J; "Applications of Artificial Intelligence for Qrganic Chemistry: The DENDRAL Project"; Mcgraw-Hill; 1980.

21. [MARBLE84] Marble, D.F.; "Geographical Information Systems: An Overview"; IEEE Pecora 9 Proceedings, Spatial Information Technologies for Remote Sensing Today and Tomorrow; October 1984; pp 18-24.

22. [MCDERMOTT82] McDermott, J.; "R1: A rule based configurer of computer systems"; Artificial Intelligence, Vol 19, No 1; September 1982, pp 39-88.

23. [MCKEOWN84] McKeown, D.M.; "Knowledge-Based Aerial Photo Interpretation"; Photogrammetrica 39; 1984; pp 91-123.

24. [MCKEOWN85] McKeown, D.M., Harvey, W.A. and McDermott, J.; "Rule Based Interpretation of Aerial Imagery"; IEEE Transactions on Pattern Analysis and Machine Intelligence, Vol PAMI-7, No 5; September 1985; pp 570-585.

25. [MURPHY83] Murphy, J., Bennett, D. and Guertin, F.; "Radiometric Calibration and Geocoded Precision Processing of LANDSAT 4 Multispectral Scanner Products by the Canada Centre for Remote Sensing"; Landsat 4 Science Characterization: Early Results, NASA Conference Publication 23-55; February 1983; pp 1.77-1.118.

26. [NASA83] Alford, W. (ed.) and Baker, S. (ed.); "LANDSAT 4 Multispectral Scanner (MSS) Subsystem Radiometric Characterization"; NASA E83-10226; February 1983.

27. [NOAA84] "LANDSAT 4 Data Users Handbook"; U.S. Geological Survey, National Oceanic and Atmospheric Administration; 1984.

28. [PARSONS84] Parsons, T.J.; "Towards Robust Image Matching Algorithms"; SPIE Vol. 504 Applications of Digital Image Processing VII; 1984; pp 436-444..

29. [PLUNKETT86] Plunkett, G.W., Goodenough, D,G, and Goldberg, M.; "Map/Image Congruency Evaluation Knowledge Based System"; Graphics/Vision Interface; May 1986; pp 273-278.

30. [RICH83] Rich, E.; "Artificial Intelligence"; Mcgraw-Hill; 1983.

31. [SCOWN85] Scown, S.J.; "The Artificial Intelligence Experience: An Introduction"; Digital Equipment Corporation; 1985.

32. [SHAPIRO80] Shapiro, L.G.; "Design of a Spatial Information System"; Map Data Processing, Freeman, H. (ed) and Pieroni, G.G. (ed); 1980; pp 101-118.

33. [SHAPIRO85] Shapiro L.G.; "The Role of AI in Computer Vision"; Proceedings of the Second Conference on Artificial Intelligence Applications, IEEE Publications; December 1985; pp 76-81.

34. [SHORTLIFFE76] Shortliffe, E.; "Computer-Based Medical Consultations: MYCIN"; Elsevier; 1976.

35. [STANSFIELD86] Stansfield, S.A.; "ANGY - A Rule-based Expert System for Automatic Segmentation of Coronary Vessels from Digital Subtracted Angiograms"; IEEE Transactions on Pattern Analysis and Machine Intelligence, Volume PAMI-8, Number 2; March 1986; pp 188-199.

36. [TSOTSOS85] Tsotsos, J.K.; "Knowledge Organization and Its Role in Representation and Interpretation for Time-Varying data: the ALVEN System"; Computational Intelligence, Vol. 1, No. 1; February 1985; pp 16-32.

37. [WINSTON84] Winston, P.H.; "Artificial Intelligence"; Second Edition, Addison-Wesley; 1984.

38. [WOODHAM85] Woodham, R.J., Catanzariti, E. and Mackworth, A.K.; "Analysis By Synthesis in Computational Vision with Applications to Remote Sensing"; Computational Intelligence, Vol 1, No 2; May 1985; pp 71-79.

39. [ZARZYCKI82] Zarzycki, J.M. and Allam, M.M.; "Canadian Council on Survey and Mapping - National Standards for the Exchange of Digital Topographic Data"; Topographical Surveys Division, Surveys and Mapping Branch; April 1982.

10 SAMPLE RUN

```
*** RESHELL V1.8 ***
LOADING : es_controller - 86/08/05  12:10:50
* Initializing System *
* Executing startup file *
* Startup file executed *
* Loading frame files *
* Frame files not defined *
* No operator knowledge present *
* Loading knowledge and context for: category_rbs *
* Loading knowledge and context for: class_rbs *
* Loading knowledge and context for: mice_rbs *
* All knowledge loaded *
* Initialized system *

 Start of The MICE SYSTEM
* Loading Map Class Information *
 Map Segment 1 class hydrography size 13
     shape 1.969E1 window [24,46,27,49]
 Map Segment 2 class hydrography size 6
     shape 1.667E1 window [57,47,59,48]
 Map Segment 3 class hydrography size 25
     shape 2.304E1 window [114,174,120,178]
 Map Segment 4 class hydrography size 22
     shape 3.073E1 window [51,112,55,117]
 Map Segment 5 class hydrography size 22
     shape 3.073E1 window [75,97,80,103]
 Map Segment 6 class hydrography size 29
     shape 2.331E1 window [29,47,35,52]
 Map Segment 7 class hydrography size 10
     shape 1.96E1 window [55,43,57,46]
 Map Segment 9 class hydrography size 8
     shape 1.8E1 window [14,212,16,214]
 Map Segment 10 class hydrography size 20
     shape 2.42E1 window [107,72,111,77]
 Map Segment 11 class hydrography size 12
     shape 2.7E1 window [168,11,172,14]
 Map Segment 12 class hydrography size 12
     shape 2.133E1 window [213,129,216,132]
 Map Segment 13 class hydrography size 29
     shape 3.986E1 window [199,145,206,152]
 Map Segment 14 class hydrography size 2506
     shape 9.861E2 window [60,51,237,273]

* Loading Image Segment Information *
 Image Segment 1 Class land_cover size 2160
     shape 1.148E2 window [1,1,240,9
 Image Segment 2 Class land_cover size 32803
     shape 1.601E2 window [1,10,240,275]
 Image Segment 3 Class hydrography size 9
     shape 2.178E1 window [1,20,3,23]
 Image Segment 4 Class land_cover size 4
     shape 1.6E1 window [1,163,2,164]
 Image Segment 5 Class land_cover size 30
```

shape 3.853E1 window [5,169,11,177]
Image Segment 6 Class land_cover size 13
shape 3.077E1 window [6,95,9,100]
Image Segment 7 Class land_cover size 14
shape 2.857E1 window [12,18,16,22]
Image Segment 8 Class land_cover size 10
shape 1.96E1 window [12,176,15,178]
Image Segment 9 Class land_cover size 18
shape 2.222E1 window [12,186,16,190]
Image Segment 10 Class land_cover size 5
shape 2.88E1 window [14,111,16,113]
Image Segment 11 Class land_cover size 57
shape 3.095E1 window [15,175,25,183]
Image Segment 12 Class land_cover size 21
shape 3.219E1 window [15,188,21,192]
Image Segment 13 Class land_cover size 8
shape 2.45E1 window [16,175,19,177]
Image Segment 14 Class land_cover size 13
shape 3.077E1 window [17,183,20,188]
Image Segment 15 Class land_cover size 2
shape 1.8E1 window [19,63,19,64]
Image Segment 16 Class land_cover size 14
shape 1.829E1 window [20,184,23,187]
Image Segment 17 Class land_cover size 15
shape 3.227E1 window [22,37,24,43]
Image Segment 18 Class land_cover size 8
shape 2.45E1 window [22,166,25,168]
Image Segment 19 Class land_cover size 14
shape 2.314E1 window [22,186,25,190]
Image Segment 20 Class land_cover size 56
shape 3.15E1 window [23,162,31,172]
Image Segment 21 Class land_cover size 5
shape 2.0E1 window [23,173,24,175]
Image Segment 22 Class land_cover size 122
shape 3.57E1 window [23,172,32,190]
Image Segment 23 Class land_cover size 12
shape 2.133E1 window [24,160,28,162]
Image Segment 24 Class land_cover size 5
shape 2.88E1 window [24,171,26,173]
Image Segment 25 Class land_cover size 13
shape 1.969E1 window [25,43,27,47]
Image Segment 26 Class land_cover size 20
shape 2.0E1 window [25,132,31,134]
Image Segment 27 Class land_cover size 9
shape 2.178E1 window [27,157,30,159]
Image Segment 28 Class land_cover size 21
shape 2.305E1 window [27,188,31,193]
Image Segment 29 Class land_cover size 40
shape 2.56E1 window [29,157,35,165]
Image Segment 30 Class land_cover size 32
shape 2.813E1 window [29,166,34,173]
Image Segment 31 Class hydrography size 16
shape 2.5E1 window [30,46,34,50]
Image Segment 32 Class land_cover size 6
shape 3.267E1 window [32,131,35,133]

Image Segment 33 Class land cover size 10
shape 1.96E1 window [35,160,37,163]
Image Segment 34 Class land cover size 12
shape 2.133E1 window [40,140,43,143]
Image Segment 35 Class land cover size 14
shape 2.314E1 window [41,142,44,146]
Image Segment 36 Class land cover size 21
shape 2.305E1 window [44,128,50,131]
Image Segment 37 Class land cover size 6
shape 2.4E1 window [47,49,50,50]
Image Segment 38 Class land cover size 19
shape 2.547E1 window [50,16,54,21]
Image Segment 39 Class land cover size 5
shape 2.0E1 window [50,41,52,42]
Image Segment 40 Class hydrography size 8
shape 1.8E1 window [52,113,54,115]
Image Segment 41 Class land cover size 9
shape 2.178E1 window [54,112,57,114]
Image Segment 42 Class land cover size 9
shape 2.844E1 window [59,129,62,132]
Image Segment 43 Class land cover size 8
shape 2.45E1 window [61,125,63,128]
Image Segment 44 Class hydrography size 11
shape 1.782E1 window [61,133,63,136]
Image Segment 45 Class hydrography size 11
shape 1.782E1 window [61,137,63,140]
Image Segment 46 Class hydrography size 12
shape 2.133E1 window [61,167,63,171]
Image Segment 47 Class hydrography size 13
shape 1.969E1 window [62,129,65,132]
Image Segment 48 Class hydrography size 7
shape 2.057E1 window [62,140,64,142]
Image Segment 49 Class land cover size 7
shape 2.057E1 window [62,146,64,148]
Image Segment 50 Class hydrography size 7
shape 2.8E1 window [62,164,64,167]
Image Segment 51 Class hydrography size 8
shape 2.45E1 window [62,171,65,173]
Image Segment 52 Class land cover size 9
shape 1.6E1 window [62,181,64,183]
Image Segment 53 Class land cover size 15
shape 2.16E1 window [63,125,67,128]
Image Segment 54 Class land cover size 26680
shape 1.463E2 window [63,54,240,275]
Image Segment 55 Class hydrography size 12
shape 2.133E1 window [63,142,66,145]
Image Segment 56 Class hydrography size 10
shape 1.96E1 window [63,162,66,164]
Image Segment 57 Class hydrography size 17
shape 2.847E1 window [63,174,68,178]
Image Segment 58 Class hydrography size 10
shape 1.96E1 window [64,159,67,161]
Image Segment 59 Class land cover size 8
shape 1.8E1 window [64,169,66,171]
Image Segment 60 Class hydrography size 8

shape 1.8E1 window [65,128,67,130]
Image Segment 61 Class hydrography size 9
shape 2.178E1 window [65,146,67,149]
Image Segment 62 Class hydrography size 28
shape 2.8E1 window [66,149,68,159]
Image Segment 63 Class hydrography size 11
shape 1.782E1 window [68,128,71,130]
Image Segment 64 Class land_cover size 6
shape 2.4E1 window [68,149,70,151]
Image Segment 65 Class hydrography size 19
shape 2.547E1 window [68,177,72,182]
Image Segment 66 Class land_cover size 10
shape 2.56E1 window [69,175,72,178]
Image Segment 67 Class hydrography size 14
shape 2.314E1 window [71,129,75,132]
Image Segment 68 Class land_cover size 9
shape 1.6E1 window [72,195,74,197]
Image Segment 69 Class hydrography size 9
shape 1.6E1 window [73,181,75,183]
Image Segment 70 Class land_cover size 12
shape 2.133E1 window [75,102,78,105]
Image Segment 71 Class hydrography size 12
shape 2.7E1 window [75,131,78,135]
Image Segment 72 Class land_cover size 8
shape 1.8E1 window [76,95,78,97]
Image Segment 73 Class hydrography size 6
shape 2.4E1 window [76,182,78,184]
Image Segment 74 Class land_cover size 16
shape 3.025E1 window [77,98,79,104]
Image Segment 75 Class land_cover size 5
shape 2.0E1 window [78,106,79,108]
Image Segment 76 Class hydrography size 8
shape 1.8E1 window [78,184,80,186]
Image Segment 77 Class hydrography size 15
shape 2.667E1 window [79,133,83,137]
Image Segment 78 Class hydrography size 9
shape 2.178E1 window [79,185,81,188]
Image Segment 79 Class hydrography size 26
shape 2.6E1 window [80,189,83,197]
Image Segment 80 Class hydrography size 9
shape 2.178E1 window [82,198,85,200]
Image Segment 81 Class hydrography size 9
shape 2.178E1 window [83,136,86,138]
Image Segment 82 Class land_cover size 9
shape 2.178E1 window [84,201,87,203]
Image Segment 83 Class land_cover size 23
shape 3.409E1 window [85,33,94,36]
Image Segment 84 Class hydrography size 18
shape 1.8E1 window [85,101,87,106]
Image Segment 85 Class hydrography size 14
shape 2.857E1 window [85,107,89,111]
Image Segment 86 Class land_cover size 8
shape 1.8E1 window [86,86,88,88]
Image Segment 87 Class hydrography size 12
shape 2.133E1 window [86,97,88,101]

Image Segment 88 Class hydrography size 19
shape 3.032E1 window [86,132,91,137]
Image Segment 89 Class land_cover size 17
shape 2.847E1 window [86,199,91,203]
Image Segment 90 Class hydrography size 24
shape 3.267E1 window [86,203,92,209]
Image Segment 91 Class hydrography size 16
shape 2.5E1 window [87,94,91,98]
Image Segment 92 Class land_cover size 18
shape 2.222E1 window [87,105,91,109]
Image Segment 93 Class hydrography size 11
shape 2.327E1 window [87,112,91,114]
Image Segment 94 Class land_cover size 10
shape 2.56E1 window [87,264,90,267]
Image Segment 95 Class land_cover size 7
shape 2.057E1 window [88,102,90,104]
Image Segment 96 Class land_cover size 11
shape 1.782E1 window [88,150,90,153]
Image Segment 97 Class land_cover size 14
shape 2.314E1 window [89,98,92,102]
Image Segment 98 Class hydrography size 19
shape 2.547E1 window [89,115,93,120]
Image Segment 99 Class hydrography size 16
shape 2.025E1 window [89,123,91,128]
Image Segment 100 Class land_cover size 10
shape 2.56E1 window [90,101,93,104]
Image Segment 101 Class hydrography size 8
shape 1.8E1 window [90,120,92,122]
Image Segment 102 Class hydrography size 14
shape 1.829E1 window [90,128,92,132]
Image Segment 103 Class hydrography size 12
shape 2.133E1 window [91,91,94,94]
Image Segment 104 Class land_cover size 7
shape 2.057E1 window [91,96,93,98]
Image Segment 105 Class land_cover size 13
shape 1.969E1 window [91,210,94,213]
Image Segment 106 Class land_cover size 6
shape 2.4E1 window [92,35,94,37]
Image Segment 107 Class land_cover size 10
shape 1.96E1 window [92,87,94,90]
Image Segment 108 Class land_cover size 18
shape 3.2E1 window [92,93,97,98]
Image Segment 109 Class land_cover size 8
shape 2.45E1 window [92,123,94,126]
Image Segment 110 Class land_cover size 4
shape 1.6E1 window [93,99,94,100]
Image Segment 111 Class hydrography size 16
shape 3.6E1 window [93,209,98,214]
Image Segment 112 Class land_cover size 7
shape 2.057E1 window [94,85,96,87]
Image Segment 113 Class land_cover size 10
shape 1.96E1 window [95,87,98,89]
Image Segment 114 Class hydrography size 11
shape 1.782E1 window [95,90,98,92]
Image Segment 115 Class land_cover size 10

shape 4.0E1 window [96,68,99,73]
Image Segment 116 Class land_cover size 8
shape 2.45E1 window [96,209,98,212]
Image Segment 117 Class land_cover size 14
shape 2.314E1 window [97,85,101,88]
Image Segment 118 Class hydrography size 12
shape 2.7E1 window [98,89,102,92]
Image Segment 119 Class land_cover size 21
shape 2.743E1 window [98,92,105,95]
Image Segment 120 Class land_cover size 9
shape 2.178E1 window [98,268,101,270]
Image Segment 121 Class land_cover size 11
shape 2.945E1 window [99,80,102,84]
Image Segment 122 Class hydrography size 17
shape 3.976E1 window [99,214,104,220]
Image Segment 123 Class land_cover size 7
shape 2.8E1 window [100,253,103,255]
Image Segment 124 Class land_cover size 22
shape 2.2E1 window [101,75,104,81]
Image Segment 125 Class land_cover size 10
shape 1.96E1 window [101,84,104,86]
Image Segment 126 Class land_cover size 9
shape 2.178E1 window [101,87,104,89]
Image Segment 127 Class land_cover size 10
shape 1.96E1 window [101,189,103,192]
Image Segment 128 Class hydrography size 12
shape 2.7E1 window [102,90,106,93]
Image Segment 129 Class land_cover size 12
shape 2.7E1 window [103,68,106,72]
Image Segment 130 Class land_cover size 4
shape 1.6E1 window [103,73,104,74]
Image Segment 131 Class land_cover size 11
shape 2.327E1 window [104,86,107,89]
Image Segment 132 Class land_cover size 13
shape 2.492E1 window [104,218,108,221]
Image Segment 133 Class hydrography size 10
shape 2.56E1 window [104,221,107,224]
Image Segment 134 Class land_cover size 19
shape 2.547E1 window [105,89,110,93]
Image Segment 135 Class hydrography size 10
shape 1.96E1 window [107,93,110,95]
Image Segment 136 Class hydrography size 15
shape 3.227E1 window [107,224,111,229]
Image Segment 137 Class land_cover size 10
shape 1.96E1 window [108,69,110,72]
Image Segment 138 Class hydrography size 18
shape 1.8E1 window [108,73,110,78]
Image Segment 139 Class hydrography size 15
shape 2.667E1 window [108,95,112,99]
Image Segment 140 Class hydrography size 8
shape 1.8E1 window [110,99,112,101]
Image Segment 141 Class hydrography size 24
shape 3.267E1 window [110,230,116,236]
Image Segment 142 Class land_cover size 8
shape 1.8E1 window [111,71,113,73]

Image Segment 143 Class hydrography size 8
shape 2.45E1 window [111,100,113,103]
Image Segment 144 Class hydrography size 10
shape 2.56E1 window [112,103,115,106]
Image Segment 145 Class land_cover size 10
shape 1.96E1 window [113,72,116,74]
Image Segment 146 Class hydrography size 18
shape 2.222E1 window [113,173,119,175]
Image Segment 147 Class hydrography size 8
shape 1.8E1 window [115,106,117,108]
Image Segment 148 Class land_cover size 13
shape 2.492E1 window [115,272,119,275]
Image Segment 149 Class land_cover size 6
shape 2.4E1 window [116,73,118,75]
Image Segment 150 Class land_cover size 7
shape 2.057E1 window [116,126,118,128]
Image Segment 151 Class land_cover size 23
shape 2.939E1 window [117,229,123,234]
Image Segment 152 Class hydrography size 14
shape 2.857E1 window [117,234,120,239]
Image Segment 153 Class hydrography size 19
shape 2.105E1 window [118,107,124,109]
Image Segment 154 Class land_cover size 8
shape 1.8E1 window [119,82,121,84]
Image Segment 155 Class hydrography size 19
shape 2.547E1 window [121,237,125,242]
Image Segment 156 Class hydrography size 27
shape 2.504E1 window [122,81,124,90]
Image Segment 157 Class hydrography size 9
shape 2.178E1 window [123,78,125,81]
Image Segment 158 Class hydrography size 18
shape 3.756E1 window [123,90,128,96]
Image Segment 159 Class hydrography size 33
shape 3.927E1 window [124,71,132,79]
Image Segment 160 Class hydrography size 9
shape 2.178E1 window [124,106,127,108]
Image Segment 161 Class land_cover size 22
shape 2.2E1 window [124,160,129,164]
Image Segment 162 Class land_cover size 25
shape 2.304E1 window [125,84,130,89]
Image Segment 163 Class land_cover size 12
shape 2.133E1 window [125,89,128,92]
Image Segment 164 Class land_cover size 9
shape 1.6E1 window [125,165,127,167]
Image Segment 165 Class land_cover size 8
shape 1.8E1 window [125,218,127,220]
Image Segment 166 Class hydrography size 20
shape 3.38E1 window [125,241,130,247]
Image Segment 167 Class hydrography size 12
shape 2.7E1 window [127,104,131,107]
Image Segment 168 Class land_cover size 15
shape 4.507E1 window [127,269,133,273]
Image Segment 169 Class land_cover size 13
shape 1.969E1 window [128,101,131,104]
Image Segment 170 Class land_cover size 23

shape 3.409E1 window [128,175,134,180]
Image Segment 171 Class hydrography size 14
shape 2.857E1 window [129,94,133,98]
Image Segment 172 Class land cover size 11
shape 2.327E1 window [129,211,132,214]
Image Segment 173 Class hydrography size 11
shape 2.327E1 window [130,247,133,250]
Image Segment 174 Class hydrography size 14
shape 2.314E1 window [131,96,133,101]
Image Segment 175 Class hydrography size 10
shape 2.56E1 window [131,102,134,105]
Image Segment 176 Class land cover size 7
shape 2.057E1 window [131,106,134,107]
Image Segment 177 Class hydrography size 15
shape 2.667E1 window [132,68,136,72]
Image Segment 178 Class land cover size 9
shape 1.6E1 window [132,140,134,142]
Image Segment 179 Class hydrography size 22
shape 2.618E1 window [132,250,136,256]
Image Segment 180 Class land cover size 12
shape 2.133E1 window [133,42,137,44]
Image Segment 181 Class land cover size 12
shape 2.7E1 window [133,161,137,164]
Image Segment 182 Class land cover size 9
shape 2.178E1 window [133,240,136,242]
Image Segment 183 Class hydrography size 16
shape 2.025E1 window [135,257,137,262]
Image Segment 184 Class land cover size 7
shape 2.057E1 window [136,58,138,60]
Image Segment 185 Class hydrography size 9
shape 2.844E1 window [136,65,139,68]
Image Segment 186 Class land cover size 15
shape 2.16E1 window [136,163,139,167]
Image Segment 187 Class land cover size 12
shape 2.7E1 window [136,192,140,195]
Image Segment 188 Class hydrography size 9
shape 1.6E1 window [136,262,138,264]
Image Segment 189 Class land cover size 13
shape 2.492E1 window [137,56,141,59]
Image Segment 190 Class hydrography size 7
shape 2.057E1 window [137,265,139,267]
Image Segment 191 Class hydrography size 19
shape 3.032E1 window [138,267,143,272]
Image Segment 192 Class hydrography size 14
shape 2.314E1 window [139,62,142,66]
Image Segment 193 Class hydrography size 19
shape 2.547E1 window [141,55,145,60]
Image Segment 194 Class hydrography size 7
shape 2.057E1 window [141,60,143,62]
Image Segment 195 Class land cover size 25
shape 1.936E1 window [141,265,146,269]
Image Segment 196 Class land cover size 9
shape 2.178E1 window [141,273,144,275]
Image Segment 197 Class hydrography size 16
shape 2.025E1 window [142,270,146,273]

Image Segment 198 Class hydrography size 9
shape 2.844E1 window [145,52,149,54]
Image Segment 199 Class hydrography size 6
shape 1.667E1 window [145,274,147,275]
Image Segment 200 Class land cover size 7
shape 2.057E1 window [146,50,148,52]
Image Segment 201 Class land cover size 7
shape 2.057E1 window [146,150,148,152]
Image Segment 202 Class land cover size 9
shape 2.178E1 window [147,146,149,149]
Image Segment 203 Class land cover size 8
shape 1.8E1 window [147,152,149,154]
Image Segment 204 Class hydrography size 12
shape 2.133E1 window [147,271,151,273]
Image Segment 205 Class land cover size 4
shape 1.6E1 window [148,274,149,275]
Image Segment 206 Class hydrography size 16
shape 2.5E1 window [149,50,153,54]
Image Segment 207 Class land cover size 6
shape 1.667E1 window [150,274,152,275]
Image Segment 208 Class land cover size 12
shape 2.133E1 window [152,184,155,187]
Image Segment 209 Class land cover size 13
shape 2.492E1 window [153,55,157,58]
Image Segment 210 Class land cover size 13
shape 2.492E1 window [153,244,157,247]
Image Segment 211 Class hydrography size 18
shape 2.689E1 window [154,51,158,56]
Image Segment 212 Class land cover size 8
shape 1.8E1 window [154,77,156,79]
Image Segment 213 Class land cover size 17
shape 2.353E1 window [154,186,158,190]
Image Segment 214 Class land cover size 9
shape 1.6E1 window [155,181,157,183]
Image Segment 215 Class land cover size 17
shape 2.847E1 window [155,202,159,207]
Image Segment 216 Class land cover size 6
shape 1.667E1 window [156,184,158,185]
Image Segment 217 Class land cover size 11
shape 2.945E1 window [156,217,158,221]
Image Segment 218 Class hydrography size 19
shape 2.547E1 window [157,55,161,60]
Image Segment 219 Class hydrography size 19
shape 2.105E1 window [157,76,159,82]
Image Segment 220 Class land cover size 20
shape 2.88E1 window [157,178,160,184]
Image Segment 221 Class land cover size 9
shape 2.178E1 window [157,187,159,190]
Image Segment 222 Class hydrography size 9
shape 1.6E1 window [158,74,160,76]
Image Segment 223 Class hydrography size 11
shape 1.782E1 window [158,83,160,86]
Image Segment 224 Class land cover size 13
shape 1.969E1 window [158,196,161,199]
Image Segment 225 Class land cover size 13

shape 1.969E1 window [158,214,161,217]
Image Segment 226 Class hydrography size 9
shape 2.178E1 window [159,71,161,74]
Image Segment 227 Class hydrography size 9
shape 2.178E1 window [160,60,162,63]
Image Segment 228 Class hydrography size 9
shape 2.178E1 window [160,68,162,71]
Image Segment 229 Class hydrography size 11
shape 2.327E1 window [160,86,163,89]
Image Segment 230 Class land cover size 43
shape 2.381E1 window [160,178,166,186]
Image Segment 231 Class land cover size 33
shape 2.376E1 window [160,209,165,216]
Image Segment 232 Class land cover size 12
shape 2.133E1 window [161,42,164,45]
Image Segment 233 Class hydrography size 17
shape 2.353E1 window [161,63,163,69]
Image Segment 234 Class land cover size 18
shape 2.222E1 window [161,194,164,199]
Image Segment 235 Class land cover size 8
shape 2.45E1 window [161,258,163,261]
Image Segment 236 Class land cover size 8
shape 1.8E1 window [162,262,164,264]
Image Segment 237 Class land cover size 7
shape 2.057E1 window [163,45,165,47]
Image Segment 238 Class hydrography size 7
shape 2.057E1 window [163,88,165,90]
Image Segment 239 Class land cover size 23
shape 3.409E1 window [163,183,169,188]
Image Segment 240 Class land cover size 11
shape 2.945E1 window [163,206,167,209]
Image Segment 241 Class land cover size 8
shape 2.45E1 window [163,256,165,259]
Image Segment 242 Class land cover size 11
shape 2.327E1 window [164,188,166,192]
Image Segment 243 Class land cover size 8
shape 2.45E1 window [164,244,166,247]
Image Segment 244 Class land cover size 20
shape 2.42E1 window [165,41,170,45]
Image Segment 245 Class hydrography size 23
shape 2.104E1 window [165,89,172,91]
Image Segment 246 Class land cover size 20
shape 2.0E1 window [165,213,170,216]
Image Segment 247 Class land cover size 10
shape 1.96E1 window [166,204,169,206]
Image Segment 248 Class land cover size 13
shape 2.492E1 window [167,92,172,94]
Image Segment 249 Class land cover size 8
shape 1.8E1 window [167,182,169,184]
Image Segment 250 Class land cover size 12
shape 2.133E1 window [167,216,170,219]
Image Segment 251 Class land cover size 12
shape 2.133E1 window [169,181,172,184]
Image Segment 252 Class land cover size 7
shape 2.057E1 window [170,213,172,215]

Image Segment 253 Class land_cover size 10
shape 1.96E1 window [171,215,173,218]
Image Segment 254 Class land_cover size 10
shape 1.96E1 window [171,249,173,252]
Image Segment 255 Class land_cover size 28
shape 2.414E1 window [172,179,176,186]
Image Segment 256 Class land_cover size 13
shape 1.969E1 window [173,88,176,91]
Image Segment 257 Class land_cover size 17
shape 2.353E1 window [174,215,179,218]
Image Segment 258 Class land_cover size 8
shape 1.8E1 window [174,246,176,248]
Image Segment 259 Class land_cover size 5
shape 2.0E1 window [174,256,176,257]
Image Segment 260 Class land_cover size 12
shape 2.133E1 window [175,171,177,175]
Image Segment 261 Class land_cover size 11
shape 1.782E1 window [175,176,177,179]
Image Segment 262 Class hydrography size 8
shape 2.45E1 window [176,87,179,89]
Image Segment 263 Class land_cover size 11
shape 1.782E1 window [177,169,180,171]
Image Segment 264 Class hydrography size 7
shape 2.057E1 window [179,86,181,88]
Image Segment 265 Class land_cover size 10
shape 2.56E1 window [179,256,183,258]
Image Segment 266 Class hydrography size 38
shape 3.042E1 window [181,75,184,87]
Image Segment 267 Class land_cover size 20
shape 2.0E1 window [181,200,186,203]
Image Segment 268 Class land_cover size 17
shape 2.353E1 window [182,203,187,206]
Image Segment 269 Class hydrography size 9
shape 2.178E1 window [183,72,185,75]
Image Segment 270 Class hydrography size 14
shape 2.314E1 window [184,68,187,72]
Image Segment 271 Class land_cover size 4
shape 1.6E1 window [184,274,185,275]
Image Segment 272 Class land_cover size 17
shape 1.906E1 window [185,81,188,85]
Image Segment 273 Class land_cover size 12
shape 2.7E1 window [186,217,189,221]
Image Segment 274 Class land_cover size 8
shape 1.8E1 window [186,220,188,222]
Image Segment 275 Class hydrography size 10
shape 2.5E1 window [188,66,190,70]
Image Segment 276 Class hydrography size 12
shape 2.133E1 window [191,65,195,67]
Image Segment 277 Class land_cover size 3
shape 2.133E1 window [192,145,193,146]
Image Segment 278 Class land_cover size 12
shape 2.133E1 window [195,37,198,40]
Image Segment 279 Class hydrography size 21
shape 2.743E1 window [196,65,202,69]
Image Segment 280 Class land_cover size 10

shape 2.56E1 window [198,222,201,225]
Image Segment 281 Class land_cover size 7
shape 2.057E1 window [199,272,201,274]
Image Segment 282 Class hydrography size 13
shape 2.492E1 window [200,70,204,73]
Image Segment 283 Class land_cover size 10
shape 1.96E1 window [200,212,203,214]
Image Segment 284 Class land_cover size 29
shape 3.531E1 window [200,211,206,219]
Image Segment 285 Class land_cover size 5
shape 2.0E1 window [200,274,202,275]
Image Segment 286 Class land_cover size 10
shape 1.96E1 window [201,224,204,226]
Image Segment 287 Class land_cover size 5
shape 2.88E1 window [201,257,203,259]
Image Segment 288 Class land_cover size 8
shape 2.45E1 window [202,68,205,70]
Image Segment 289 Class land_cover size 6
shape 2.4E1 window [202,210,204,212]
Image Segment 290 Class hydrography size 21
shape 3.733E1 window [203,73,208,80]
Image Segment 291 Class land_cover size 13
shape 2.492E1 window [205,70,208,74]
Image Segment 292 Class land_cover size 14
shape 2.314E1 window [207,74,211,77]
Image Segment 293 Class hydrography size 21
shape 2.743E1 window [209,78,214,83]
Image Segment 294 Class land_cover size 20
shape 2.42E1 window [210,76,216,79]
Image Segment 295 Class land_cover size 23
shape 3.913E1 window [212,103,219,109]
Image Segment 296 Class land_cover size 9
shape 1.6E1 window [213,129,215,131]
Image Segment 297 Class land_cover size 9
shape 1.6E1 window [214,202,216,204]
Image Segment 298 Class hydrography size 16
shape 2.5E1 window [215,80,219,84]
Image Segment 299 Class land_cover size 10
shape 1.96E1 window [216,78,219,80]
Image Segment 300 Class land_cover size 26
shape 2.215E1 window [217,211,222,216]
Image Segment 301 Class land_cover size 14
shape 2.314E1 window [219,79,224,81]
Image Segment 302 Class hydrography size 9
shape 1.6E1 window [220,82,222,84]
Image Segment 303 Class land_cover size 10
shape 2.56E1 window [220,101,223,104]
Image Segment 304 Class hydrography size 9
shape 2.178E1 window [223,81,226,83]
Image Segment 305 Class land_cover size 25
shape 3.136E1 window [226,74,232,80]
Image Segment 306 Class hydrography size 12
shape 2.133E1 window [227,79,230,82]
Image Segment 307 Class land_cover size 6
shape 2.4E1 window [231,17,233,19]

```
Image Segment 308 Class land_cover size 29
    shape 2.331E1 window [231,61,234,69]
Image Segment 309 Class hydrography size 11
    shape 1.782E1 window [231,78,234,80]
Image Segment 310 Class hydrography size 15
    shape 2.16E1 window [232,73,235,77]
Image Segment 311 Class land_cover size 14
    shape 2.314E1 window [233,95,236,99]
Image Segment 312 Class land_cover size 16
    shape 2.025E1 window [233,224,236,228]
Image Segment 313 Class hydrography size 43
    shape 3.014E1 window [234,60,237,73]
Image Segment 314 Class land_cover size 86
    shape 3.912E1 window [235,58,240,80]
Image Segment 315 Class land_cover size 8
    shape 2.45E1 window [236,53,239,55]
Image Segment 316 Class hydrography size 19
    shape 2.547E1 window [236,54,240,59]
Image Segment 317 Class land_cover size 10
    shape 1.96E1 window [238,50,240,53]
Image Segment 318 Class land_cover size 7
    shape 2.057E1 window [238,139,240,141]
Image Segment 319 Class land_cover size 6
    shape 2.4E1 window [238,223,240,225]


mice - the next class selected is hydrography
map class hydrography area = 2714
image class hydrography area = 1632
mice - the next category selected is coastal_feature

the next map segment selected is 2
the image segments selected are [2]
classes mapseg = 2
the image segments in the same map class are [].
* Marking Results *
image segments of similar size are []
* Marking Results *
the image segments shapes are []
* Marking Results *
the image segments overlap are [2]
* Marking Results *

the next map segment selected is 9
the image segments selected are [2]
the image segments in the same map class are []
* Marking Results *
image segments of similar size are []
* Marking Results *
the image segments shapes are []
* Marking Results *
the image segments overlap are [2]
* Marking Results *

the next map segment selected is 7
```

```
 the image segments selected are [2]
 the image segments in the same map class are [ ]
* Marking Results *
 image segments of similar size are [ ]
* Marking Results *
 the image segments shapes are [ ]
* Marking Results *
 the image segments overlap are [2]
* Marking Results *

 the next map segment selected is 11
 the image segments selected are [2]
 the image segments in the same map class are [ ]
* Marking Results *
 image segments of similar size are [ ]
* Marking Results *
 the image segments shapes are [ ]
* Marking Results *
 the image segments overlap are [2]
* Marking Results *

 the next map segment selected is 12
 the image segments selected are [2,54,296]
 the image segments in the same map class are [ ]
* Marking Results *
 image segments of similar size are [296]
* Marking Results *
 the image segments shapes are [296]
* Marking Results *
 the image segments overlap are [296,54]
* Marking Results *

 the next map segment selected is 1
 the image segments selected are [2,25]
 the image segments in the same map class are [ ]
* Marking Results *
 image segments of similar size are [25]
* Marking Results *
 the image segments shapes are [25]
* Marking Results *
 the image segments overlap are [25,2]
* Marking Results *

 the next map segment selected is 10
 the image segments selected are [2,54,129,137,
     138,142,145]
 the image segments in the same map class are [138]
* Marking Results *
 image segments of similar size are [138]
* Marking Results *
 the image segments shapes are [145,142,138,137,129]
* Marking Results *
 the image segments overlap are [138,2]
* Marking Results *
```

```
 the next map segment selected is 4
 the image segments selected are [2,40,41]
 the image segments in the same map class are [40]
* Marking Results *
 image segments of similar size are []
* Marking Results *
 the image segments shapes are [41]
* Marking Results *
 the image segments overlap are [41,40,2]
* Marking Results *

 the next map segment selected is 5
 the image segments selected are [2,54,70,72,74,75]
 the image segments in the same map class are []
* Marking Results *
 image segments of similar size are [74]
* Marking Results *
 the image segments shapes are [74,70]
* Marking Results *
 the image segments overlap are [74,72,70,2]
* Marking Results *

 the next map segment selected is 3
 the image segments selected are [2,54,146]
 the image segments in the same map class are [146]
* Marking Results *
 image segments of similar size are [146]
* Marking Results *
 the image segments shapes are [146]
* Marking Results *
 the image segments overlap are [146,54]
* Marking Results *

 the next map segment selected is 6
 the image segments selected are [2,25,31]
 the image segments in the same map class are [31]
* Marking Results *
 image segments of similar size are []
* Marking Results *
 the image segments shapes are [31,25]
* Marking Results *
 the image segments overlap are [31,2]
* Marking Results *

 the next map segment selected is 13
 the image segments selected are [2,54]
 the image segments in the same map class are []
* Marking Results *
 image segments of similar size are []
* Marking Results *
 the image segments shapes are []
* Marking Results *
 the image segments overlap are [54]
* Marking Results *
```

```
the next map segment selected is 14
the image segments selected are [2,34,35,36,37,
   39,40,41,42,43,44,45,46,47,48,49,50,51,52,
   53,54,55,56,57,58,59,60,61,62,63,64,65,66,
   67,68,69,70,71,72,73,74,75,76,77,78,79,80,
   81,82,83,84,85,86,87,88,89,90,91,92,93,94,
   95,96,97,98,99,100,101,102,103,104,105,106,
   107,108,109,110,111,112,113,114,115,116,117,
   118,119,120,121,122,123,124,125,126,127,128,
   129,130,131,132,133,134,135,136,137,138,139,
   140,141,142,143,144,145,146,147,148,149,150,
   151,152,153,154,155,156,157,158,159,160,161,
   162,163,164,165,166,167,168,169,170,171,172,
   173,174,175,176,177,178,179,180,181,182,183,
   184,185,186,187,188,189,190,191,192,193,194,
   195,196,197,198,199,200,201,202,203,204,205,
   206,207,208,209,210,211,212,213,214,215,216,
   217,218,219,220,221,222,223,224,225,226,227,
   228,229,230,231,232,233,234,235,236,237,238,
   239,240,241,242,243,244,245,246,247,248,249,
   250,251,252,253,254,255,256,257,258,259,260,
   261,262,263,264,265,266,267,268,269,270,271,
   272,273,274,275,276,277,278,279,280,281,282,
   283,284,285,286,287,288,289,290,291,292,293,
   294,295,296,297,298,299,300,301,302,303,304,
   305,306,308,309,310,311,312,313,314,315,316,
   317,318,319]
the image segments in the same map class are [316,
   313,310,309,306,304,302,298,293,290,282,279,
   276,275,270,269,266,264,262,245,238,233,229,
   228,227,226,223,222,219,218,211,206,204,199,
   198,197,194,193,192,191,190,188,185,183,179,
   177,175,174,173,171,167,166,160,159,158,157,
   156,155,153,152,147,146,144,143,141,140,139,
   138,136,135,133,128,122,118,114,111,103,102,
   101,99,98,93,91,90,88,87,85,84,81,80,79,78,77,
   76,73,71,69,67,65,63,62,61,60,58,57,56,55,51,
   50,48,47,46,45,44,40]
* Marking Results *
image segments of similar size are []
* Marking Results *
the image segments shapes are []
* Marking Results *
the image segments overlap are [316,314,313,310,
   309,306,304,302,298,294,293,292,291,290,288,
   282,279,276,275,272,270,269,266,264,262,256,
   248,245,238,233,229,228,227,226,223,222,219,
   218,211,209,206,204,198,197,196,195,194,193,
   192,191,190,189,188,185,184,183,179,177,176,
   175,174,173,171,169,167,166,163,162,160,159,
   158,157,156,155,154,153,152,147,144,143,141,
   140,139,136,135,134,133,132,131,128,126,125,
   122,119,118,117,114,113,112,111,110,109,108,
   107,105,104,103,102,101,100,99,98,97,95,93,92,
   91,90,88,87,85,84,82,81,80,79,78,77,76,73,71,
```

```
   69,67,65,63,62,61,60,58,57,56,55,54,51,50,49,
   48,47,46,45,44,42,2]
* Marking Results *

the next map segment selected is done
mice - the next category selected is
   inland_water_body

the next map segment selected is done
mice - the next category selected is
   water_course

the next map segment selected is done
mice - the next category selected is
   ground_water_feature

the next map segment selected is done
mice - the next category selected is
   wetlands

the next map segment selected is done
mice - the next category selected is
   related_hydrographic_feat

the next map segment selected is done
mice - the next category selected is
   frozen_hydrographic_feat

the next map segment selected is done
mice - the next category selected is
   done


mice - the next class selected is road_and_rail

the next map segment selected is done
mice - the next category selected is
   roadway

the next map segment selected is done
mice - the next category selected is
   through_rail_line

the next map segment selected is done
mice - the next category selected is
   done


mice - the next class selected is utility
mice - the next category selected is
   utility

the next map segment selected is done
mice - the next category selected is
   done
```

```
mice - the next class selected is land_cover
mice - the next category selected is
   woodland

the next map segment selected is done
mice - the next category selected is
   cultivated_land

the next map segment selected is done
mice - the next category selected is
   grassland

the next map segment selected is done
mice - the next category selected is
   low_vegitation

the next map segment selected is done
mice - the next category selected is
   no_vegitation

the next map segment selected is done
mice - the next category selected is
   done


mice - the next class selected is hypsography
mice - the next category selected is
   hypsography

the next map segment selected is done
mice - the next category selected is
   done


mice - the next class selected is structures
mice - the next category selected is
   structures

the next map segment selected is done
mice - the next category selected is
   done


mice - the next class selected is buildings
mice - the next category selected is
   buildings

the next map segment selected is done
mice - the next category selected is
   done


mice - the next class selected is designated_areas
```

```
mice - the next category selected is
   designated_areas

the next map segment selected is done
mice - the next category selected is
   done


mice - the next class selected is delimeters
mice - the next category selected is
   delimeters

the next map segment selected is done
mice - the next category selected is
   done


mice - the next class selected is text
mice - the next category selected is
   text

the next map segment selected is done
mice - the next category selected is
   done


mice - the next class selected is done
all classes done
```

INDEX